The interplay between the LHC and DIS experiments in probing SMEFT

Radja Boughezal

Argonne National Laboratory

Status of the Standard Model

Example: Higgs production and decay

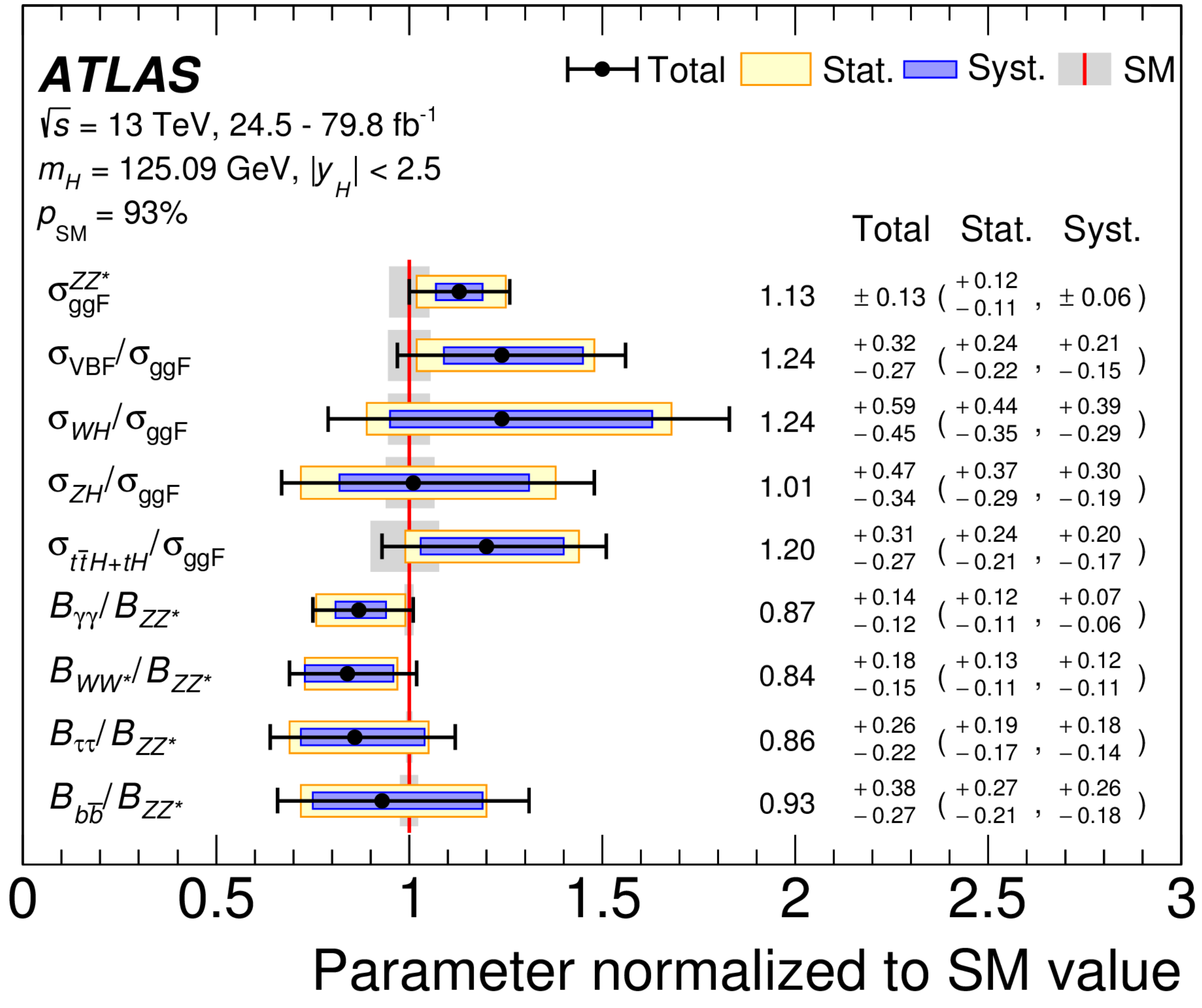

Example: di-boson cross sections

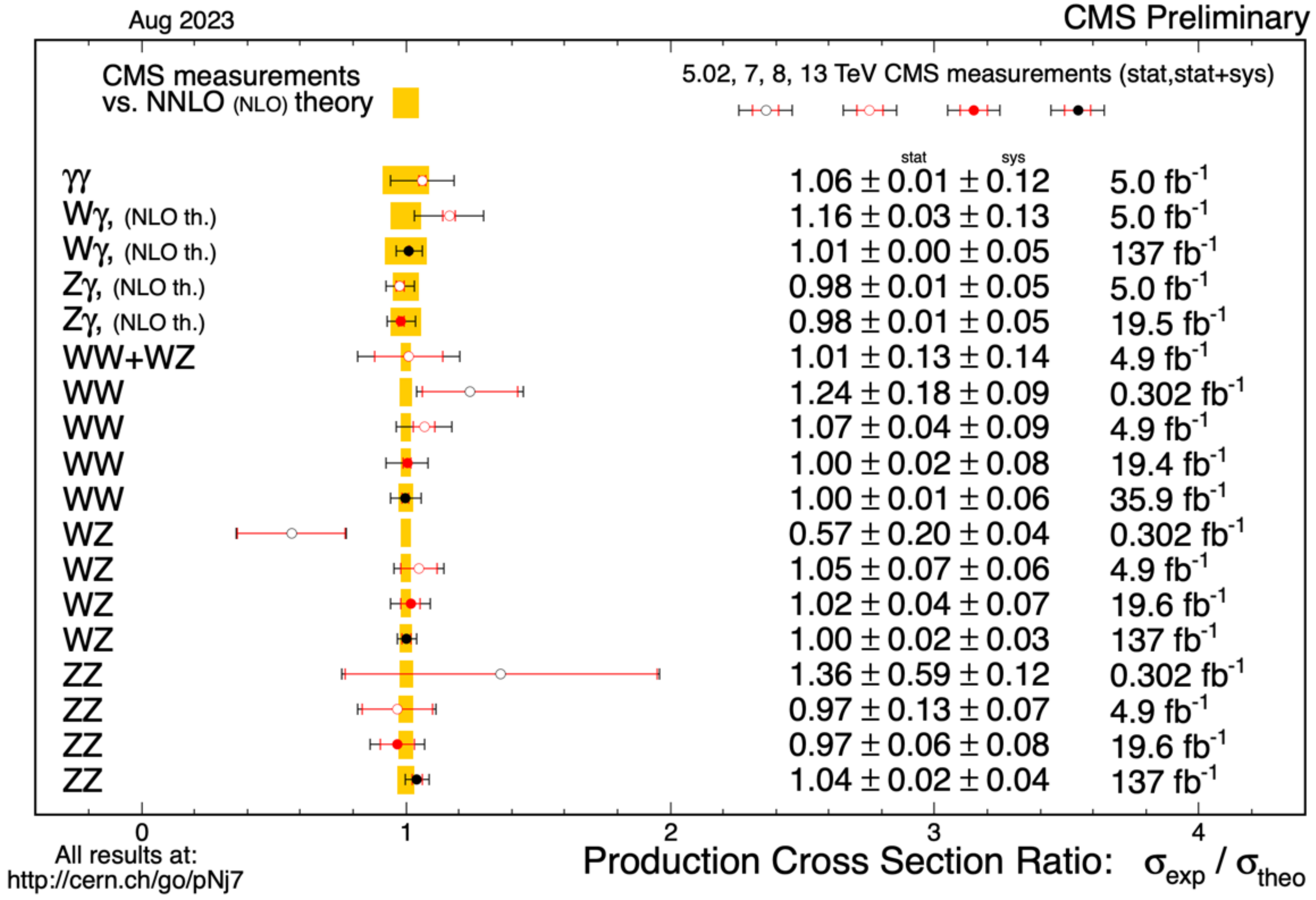

Remarkable agreement between SM theory and experiment over all sectors of the theory, and spanning orders of magnitude in cross section

LHC searches for new physics

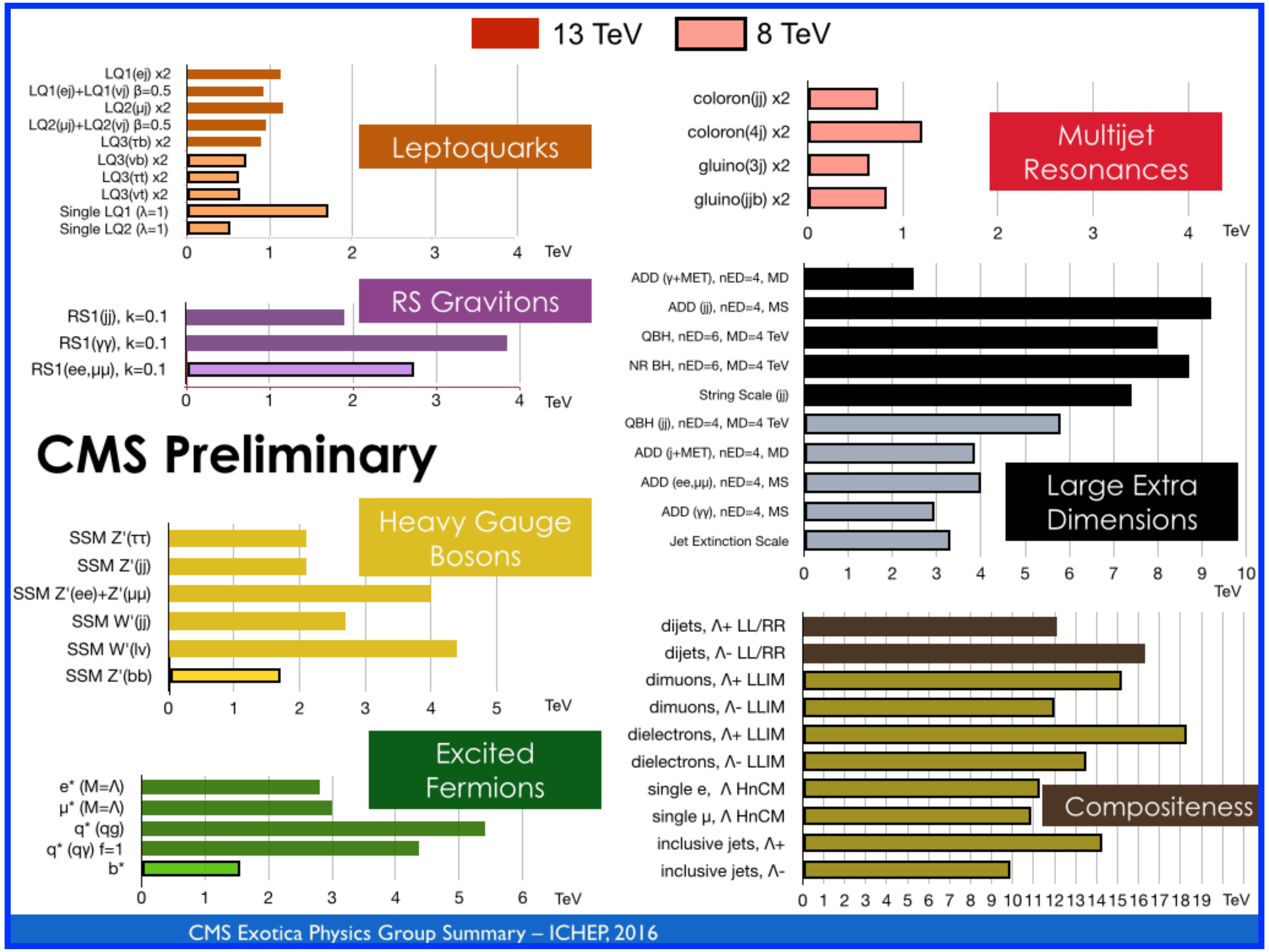

No conclusive evidence of BSM physics so far, despite a broad spectrum of searches.
Limits on new physics mass scale exceed several TeV in many cases

The heavy new physics paradigm

What do we learn from the remarkable success of the SM, combined with the null searches so far at the LHC and elsewhere?

The data suggests (although it doesn't require) a mass gap between the SM and any new physics

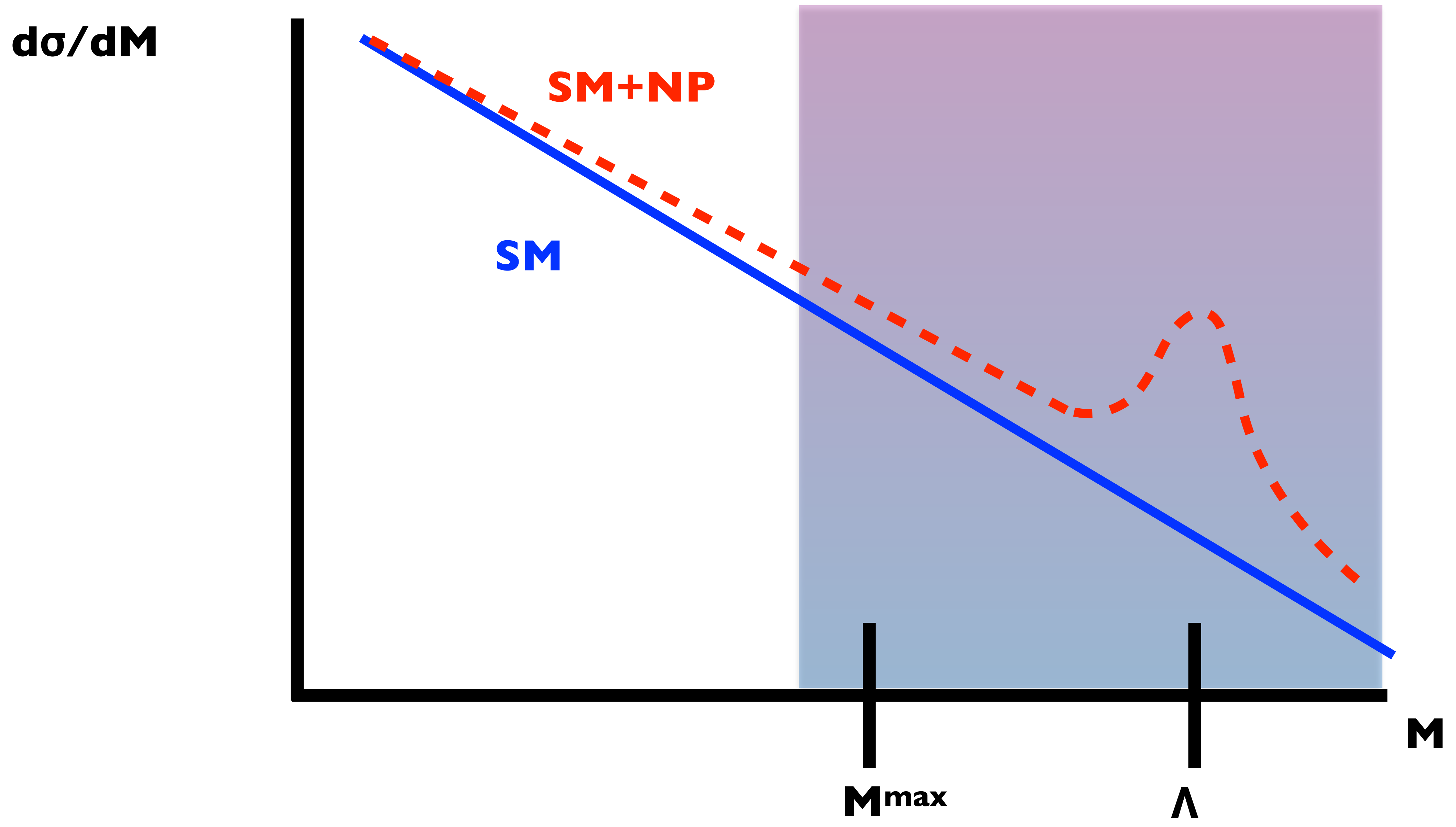

- M^{max} is the maximum energy probed at the LHC and elsewhere
- Λ is the scale where new particles appear

Hopefully Λ isn't too far above M^{max}!

Introduction to the SMEFT

- An EFT framework that incorporates this point is the Standard Model Effective Field Theory (SMEFT): assume the SM field content and gauge symmetry, and include all possible higher-dimensional operators suppressed by a scale Λ

$$\mathcal{L} = \mathcal{L}_{SM} + \frac{1}{\Lambda^2}\sum_i C_6^i(\mu)\mathcal{O}_6^i(\mu) + \frac{1}{\Lambda^4}\sum_i C_8^i(\mu)\mathcal{O}_8^i(\mu) + \ldots$$

Dimension-6 Dimension-8

- $\Lambda \gg E, v$ (Higgs vev) must both be satisfied
- Odd dimensions violate lepton or baryon number; neglected here
- RG running important when comparing experiments at disparate energies

Constructing the SMEFT

- First step is to construct a complete and non-redundant basis of operators at each dimension. One commonly-used possibility at dimension-6 is the Warsaw basis.

Buchmuller, Wyler (1986); Grzadkowski et al (2010); Brivio, Jiang, Trott (2017)

Pure Gauge interactions

Accommodates a rich phenomenology in all sectors

X^3		φ^6 and $\varphi^4 D^2$		$\psi^2\varphi^3$	
Q_G	$f^{ABC} G_\mu^{A\nu} G_\nu^{B\rho} G_\rho^{C\mu}$	Q_φ	$(\varphi^\dagger\varphi)^3$	$Q_{e\varphi}$	$(\varphi^\dagger\varphi)(\bar l_p e_r \varphi)$
$Q_{\widetilde G}$	$f^{ABC} \widetilde G_\mu^{A\nu} G_\nu^{B\rho} G_\rho^{C\mu}$	$Q_{\varphi\Box}$	$(\varphi^\dagger\varphi)\Box(\varphi^\dagger\varphi)$	$Q_{u\varphi}$	$(\varphi^\dagger\varphi)(\bar q_p u_r \widetilde\varphi)$
Q_W	$\varepsilon^{IJK} W_\mu^{I\nu} W_\nu^{J\rho} W_\rho^{K\mu}$	$Q_{\varphi D}$	$(\varphi^\dagger D^\mu\varphi)^* (\varphi^\dagger D_\mu\varphi)$	$Q_{d\varphi}$	$(\varphi^\dagger\varphi)(\bar q_p d_r \varphi)$
$Q_{\widetilde W}$	$\varepsilon^{IJK} \widetilde W_\mu^{I\nu} W_\nu^{J\rho} W_\rho^{K\mu}$				

$X^2\varphi^2$		$\psi^2 X\varphi$		$\psi^2\varphi^2 D$	
$Q_{\varphi G}$	$\varphi^\dagger\varphi\, G^A_{\mu\nu} G^{A\mu\nu}$	Q_{eW}	$(\bar l_p \sigma^{\mu\nu} e_r)\tau^I \varphi W^I_{\mu\nu}$	$Q_{\varphi l}^{(1)}$	$(\varphi^\dagger i\overleftrightarrow{D}_\mu \varphi)(\bar l_p \gamma^\mu l_r)$
$Q_{\varphi\widetilde G}$	$\varphi^\dagger\varphi\, \widetilde G^A_{\mu\nu} G^{A\mu\nu}$	Q_{eB}	$(\bar l_p \sigma^{\mu\nu} e_r)\varphi B_{\mu\nu}$	$Q_{\varphi l}^{(3)}$	$(\varphi^\dagger i\overleftrightarrow{D}^I_\mu \varphi)(\bar l_p \tau^I \gamma^\mu l_r)$
$Q_{\varphi W}$	$\varphi^\dagger\varphi\, W^I_{\mu\nu} W^{I\mu\nu}$	Q_{uG}	$(\bar q_p \sigma^{\mu\nu} T^A u_r)\widetilde\varphi\, G^A_{\mu\nu}$	$Q_{\varphi e}$	$(\varphi^\dagger i\overleftrightarrow{D}_\mu \varphi)(\bar e_p \gamma^\mu e_r)$
$Q_{\varphi\widetilde W}$	$\varphi^\dagger\varphi\, \widetilde W^I_{\mu\nu} W^{I\mu\nu}$	Q_{uW}	$(\bar q_p \sigma^{\mu\nu} u_r)\tau^I \widetilde\varphi\, W^I_{\mu\nu}$	$Q_{\varphi q}^{(1)}$	$(\varphi^\dagger i\overleftrightarrow{D}_\mu \varphi)(\bar q_p \gamma^\mu q_r)$
$Q_{\varphi B}$	$\varphi^\dagger\varphi\, B_{\mu\nu} B^{\mu\nu}$	Q_{uB}	$(\bar q_p \sigma^{\mu\nu} u_r)\widetilde\varphi\, B_{\mu\nu}$	$Q_{\varphi q}^{(3)}$	$(\varphi^\dagger i\overleftrightarrow{D}^I_\mu \varphi)(\bar q_p \tau^I \gamma^\mu q_r)$
$Q_{\varphi\widetilde B}$	$\varphi^\dagger\varphi\, \widetilde B_{\mu\nu} B^{\mu\nu}$	Q_{dG}	$(\bar q_p \sigma^{\mu\nu} T^A d_r)\varphi\, G^A_{\mu\nu}$	$Q_{\varphi u}$	$(\varphi^\dagger i\overleftrightarrow{D}_\mu \varphi)(\bar u_p \gamma^\mu u_r)$
$Q_{\varphi WB}$	$\varphi^\dagger\tau^I\varphi\, W^I_{\mu\nu} B^{\mu\nu}$	Q_{dW}	$(\bar q_p \sigma^{\mu\nu} d_r)\tau^I \varphi\, W^I_{\mu\nu}$	$Q_{\varphi d}$	$(\varphi^\dagger i\overleftrightarrow{D}_\mu \varphi)(\bar d_p \gamma^\mu d_r)$
$Q_{\varphi\widetilde WB}$	$\varphi^\dagger\tau^I\varphi\, \widetilde W^I_{\mu\nu} B^{\mu\nu}$	Q_{dB}	$(\bar q_p \sigma^{\mu\nu} d_r)\varphi\, B_{\mu\nu}$	$Q_{\varphi ud}$	$i(\widetilde\varphi^\dagger D_\mu\varphi)(\bar u_p \gamma^\mu d_r)$

$(\bar LL)(\bar LL)$		$(\bar RR)(\bar RR)$		$(\bar LL)(\bar RR)$	
Q_{ll}	$(\bar l_p \gamma_\mu l_r)(\bar l_s \gamma^\mu l_t)$	Q_{ee}	$(\bar e_p \gamma_\mu e_r)(\bar e_s \gamma^\mu e_t)$	Q_{le}	$(\bar l_p \gamma_\mu l_r)(\bar e_s \gamma^\mu e_t)$
$Q_{qq}^{(1)}$	$(\bar q_p \gamma_\mu q_r)(\bar q_s \gamma^\mu q_t)$	Q_{uu}	$(\bar u_p \gamma_\mu u_r)(\bar u_s \gamma^\mu u_t)$	Q_{lu}	$(\bar l_p \gamma_\mu l_r)(\bar u_s \gamma^\mu u_t)$
$Q_{qq}^{(3)}$	$(\bar q_p \gamma_\mu \tau^I q_r)(\bar q_s \gamma^\mu \tau^I q_t)$	Q_{dd}	$(\bar d_p \gamma_\mu d_r)(\bar d_s \gamma^\mu d_t)$	Q_{ld}	$(\bar l_p \gamma_\mu l_r)(\bar d_s \gamma^\mu d_t)$
$Q_{lq}^{(1)}$	$(\bar l_p \gamma_\mu l_r)(\bar q_s \gamma^\mu q_t)$	Q_{eu}	$(\bar e_p \gamma_\mu e_r)(\bar u_s \gamma^\mu u_t)$	Q_{qe}	$(\bar q_p \gamma_\mu q_r)(\bar e_s \gamma^\mu e_t)$
$Q_{lq}^{(3)}$	$(\bar l_p \gamma_\mu \tau^I l_r)(\bar q_s \gamma^\mu \tau^I q_t)$	Q_{ed}	$(\bar e_p \gamma_\mu e_r)(\bar d_s \gamma^\mu d_t)$	$Q_{qu}^{(1)}$	$(\bar q_p \gamma_\mu q_r)(\bar u_s \gamma^\mu u_t)$
		$Q_{ud}^{(1)}$	$(\bar u_p \gamma_\mu u_r)(\bar d_s \gamma^\mu d_t)$	$Q_{qu}^{(8)}$	$(\bar q_p \gamma_\mu T^A q_r)(\bar u_s \gamma^\mu T^A u_t)$
		$Q_{ud}^{(8)}$	$(\bar u_p \gamma_\mu T^A u_r)(\bar d_s \gamma^\mu T^A d_t)$	$Q_{qd}^{(1)}$	$(\bar q_p \gamma_\mu q_r)(\bar d_s \gamma^\mu d_t)$
				$Q_{qd}^{(8)}$	$(\bar q_p \gamma_\mu T^A q_r)(\bar d_s \gamma^\mu T^A d_t)$

$(\bar LR)(\bar RL)$ and $(\bar LR)(\bar LR)$		B-violating	
Q_{ledq}	$(\bar l_p^j e_r)(\bar d_s q_t^j)$	Q_{duq}	$\varepsilon^{\alpha\beta\gamma}\varepsilon_{jk}\left[(d_p^\alpha)^T C u_r^\beta\right]\left[(q_s^{\gamma j})^T C l_t^k\right]$
$Q_{quqd}^{(1)}$	$(\bar q_p^j u_r)\varepsilon_{jk}(\bar q_s^k d_t)$	Q_{qqu}	$\varepsilon^{\alpha\beta\gamma}\varepsilon_{jk}\left[(q_p^{\alpha j})^T C q_r^{\beta k}\right]\left[(u_s^\gamma)^T C e_t\right]$
$Q_{quqd}^{(8)}$	$(\bar q_p^j T^A u_r)\varepsilon_{jk}(\bar q_s^k T^A d_t)$	Q_{qqq}	$\varepsilon^{\alpha\beta\gamma}\varepsilon_{jn}\varepsilon_{km}\left[(q_p^{\alpha j})^T C q_r^{\beta k}\right]\left[(q_s^{\gamma m})^T C l_t^n\right]$
$Q_{lequ}^{(1)}$	$(\bar l_p^j e_r)\varepsilon_{jk}(\bar q_s^k u_t)$	Q_{duu}	$\varepsilon^{\alpha\beta\gamma}\left[(d_p^\alpha)^T C u_r^\beta\right]\left[(u_s^\gamma)^T C e_t\right]$
$Q_{lequ}^{(3)}$	$(\bar l_p^j \sigma_{\mu\nu} e_r)\varepsilon_{jk}(\bar q_s^k \sigma^{\mu\nu} u_t)$		

Gauge-Higgs interactions

Fermion-Higgs-gauge interactions

Four-fermion interactions

Baryon-number violating interactions

Constructing the SMEFT

- First step is to construct a complete and non-redundant basis of operators at each dimension. One commonly-used possibility at dimension-6 is the Warsaw basis.

Buchmuller, Wyler (1986);
Grzadkowski et al (2010);
Brivio, Jiang, Trott (2017)

Pure Gauge interactions

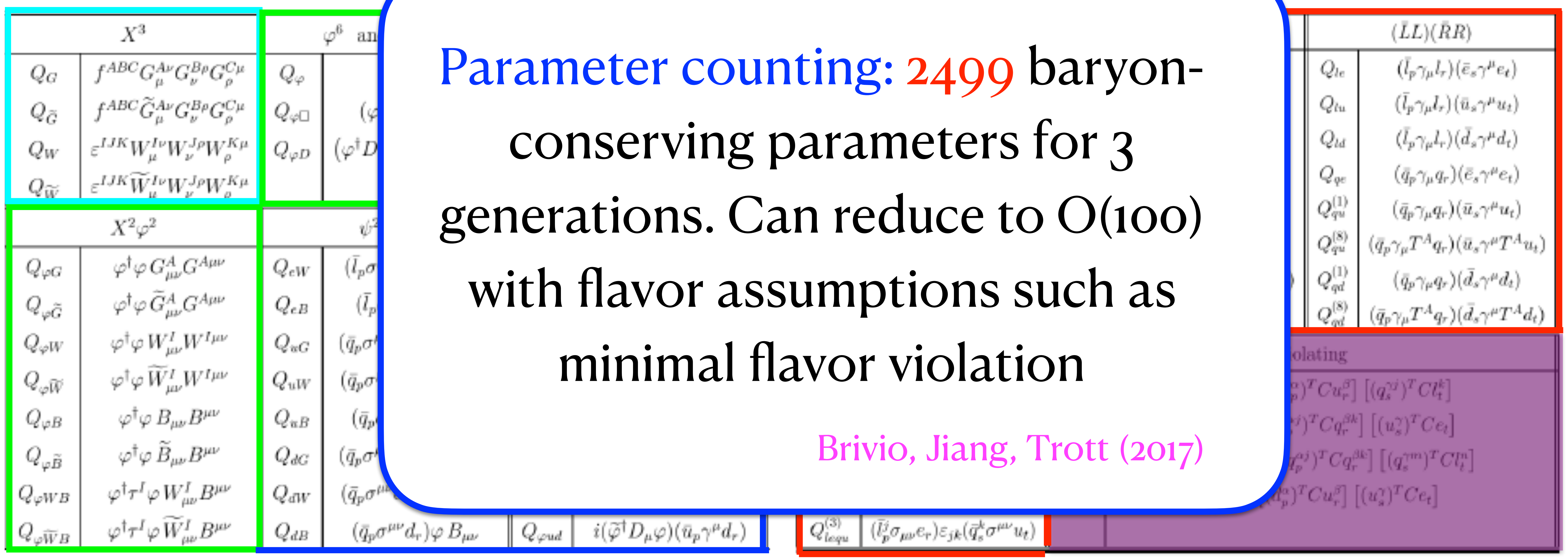

Parameter counting: 2499 baryon-conserving parameters for 3 generations. Can reduce to O(100) with flavor assumptions such as minimal flavor violation

Brivio, Jiang, Trott (2017)

Gauge-Higgs interactions

Fermion-Higgs-gauge interactions

Four-fermion interactions

Baryon-number violating interactions

Constructing the SMEFT

- First step is to construct a complete and non-redundant basis of operators at each dimension. One commonly-used possibility at dimension-6 is the Warsaw basis.

Buchmuller, Wyler (1986);
Grzadkowski et al (2010);
Brivio, Jiang, Trott (2017)

Pure Gauge interactions

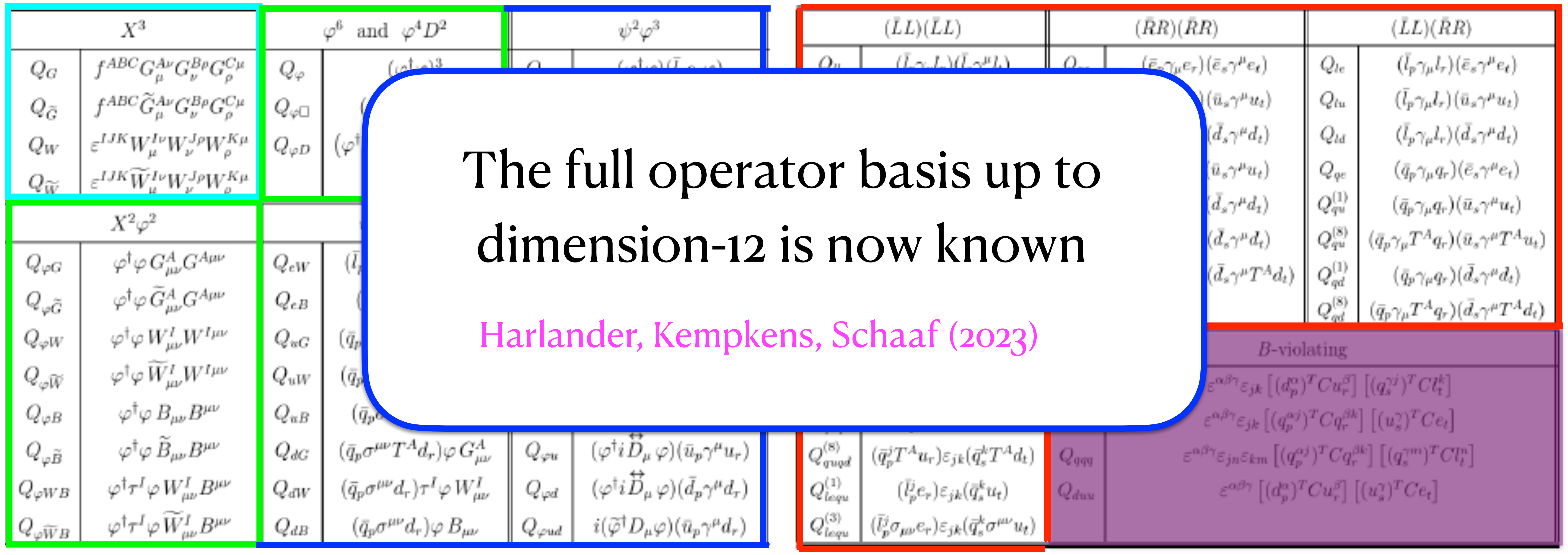

The full operator basis up to dimension-12 is now known

Harlander, Kempkens, Schaaf (2023)

Gauge-Higgs interactions

Fermion-Higgs-gauge interactions

Four-fermion interactions

Baryon-number violating interactions

Constructing the SMEFT

- We can match explicit BSM models to the EFT in a straightforward way. Each model leads to different patterns of Wilson coefficients.

Example 1:

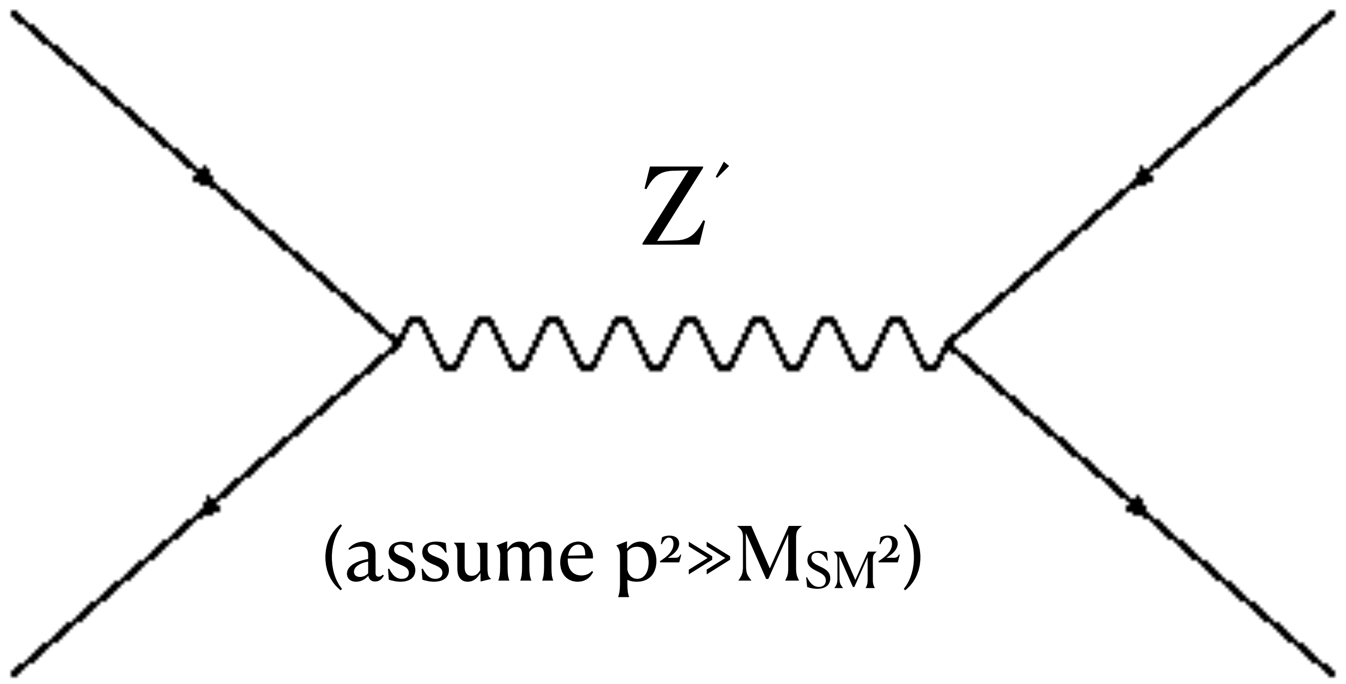

$$\sim -\frac{g_{Z'}^2}{p^2 - M_{Z'}^2} \approx \underbrace{\frac{g_{Z'}^2}{M_{Z'}^2}}_{\text{dim-6}} + \underbrace{\frac{g_{Z'}^2 p^2}{M_{Z'}^4}}_{\text{dim-8}} + \dots$$

$$\sigma \sim |\mathcal{M}_{SM}|^2 + \frac{1}{\Lambda^2} 2\mathrm{Re}\left[\mathcal{M}_6 \mathcal{M}_{SM}^*\right] + \frac{1}{\Lambda^4}\left\{|\mathcal{M}_6|^2 + 2\mathrm{Re}\left[\mathcal{M}_8 \mathcal{M}_{SM}^*\right]\right\}$$

$$|\mathcal{M}_{SM}|^2 \rightarrow \frac{g_{SM}^4}{p^4}, \quad \mathcal{M}_6 \mathcal{M}_{SM}^* \rightarrow \frac{g_{SM}^2 g_{Z'}^2}{p^2 M_{Z'}^2}, \quad |\mathcal{M}_6|^2 \rightarrow \frac{g_{Z'}^4}{M_{Z'}^4}, \quad \mathcal{M}_8 \mathcal{M}_{SM}^* \rightarrow \frac{g_{SM}^2 g_{Z'}^2}{M_{Z'}^4}$$

Constructing the SMEFT

- We can match explicit models to the EFT in a straightforward way. Each model leads to different patterns of Wilson coefficients. Measurements of the coefficients can help determine the underlying theory.

Example 2:

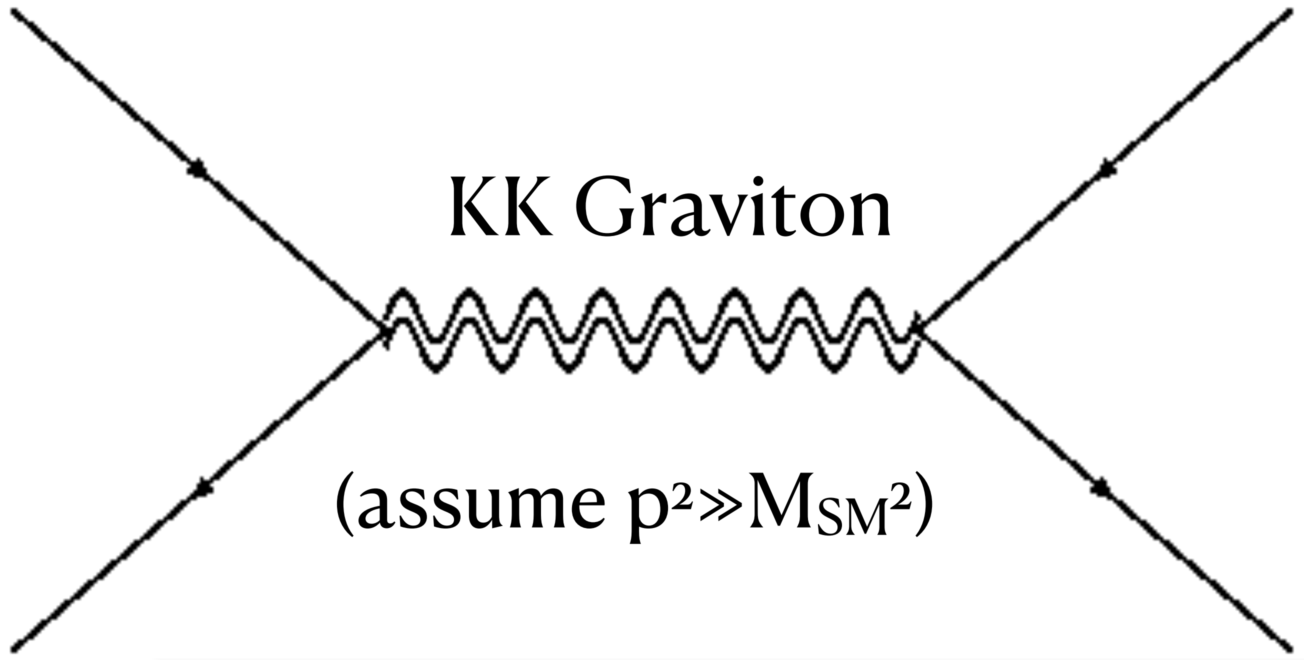

dim-6 ↓ dim-8 ↓

$$\sim 0 + \frac{p^2}{M_S^4} + \ldots$$

Han, Lykken, Zhang (1998)

$$\sigma \sim |\mathcal{M}_{SM}|^2 + \frac{1}{\Lambda^2} 2\mathrm{Re}\left[\mathcal{M}_6 \mathcal{M}_{SM}^*\right] + \frac{1}{\Lambda^4}\left\{|\mathcal{M}_6|^2 + 2\mathrm{Re}\left[\mathcal{M}_8 \mathcal{M}_{SM}^*\right]\right\}$$

$$\frac{g_{SM}^4}{p^4} \qquad 0 \qquad 0 \qquad \frac{g_{SM}^2}{M_S^4}$$

Note the very different pattern of dim-6 versus dim-8 coefficients!

Terms beyond O(1/Λ²) required for reliable predictions

Constructing the SMEFT

- We can match explicit models to the EFT in a straightforward way. Each model leads to different patterns of Wilson coefficients. Measurements of the coefficients can help determine the underlying theory.

Example 2:

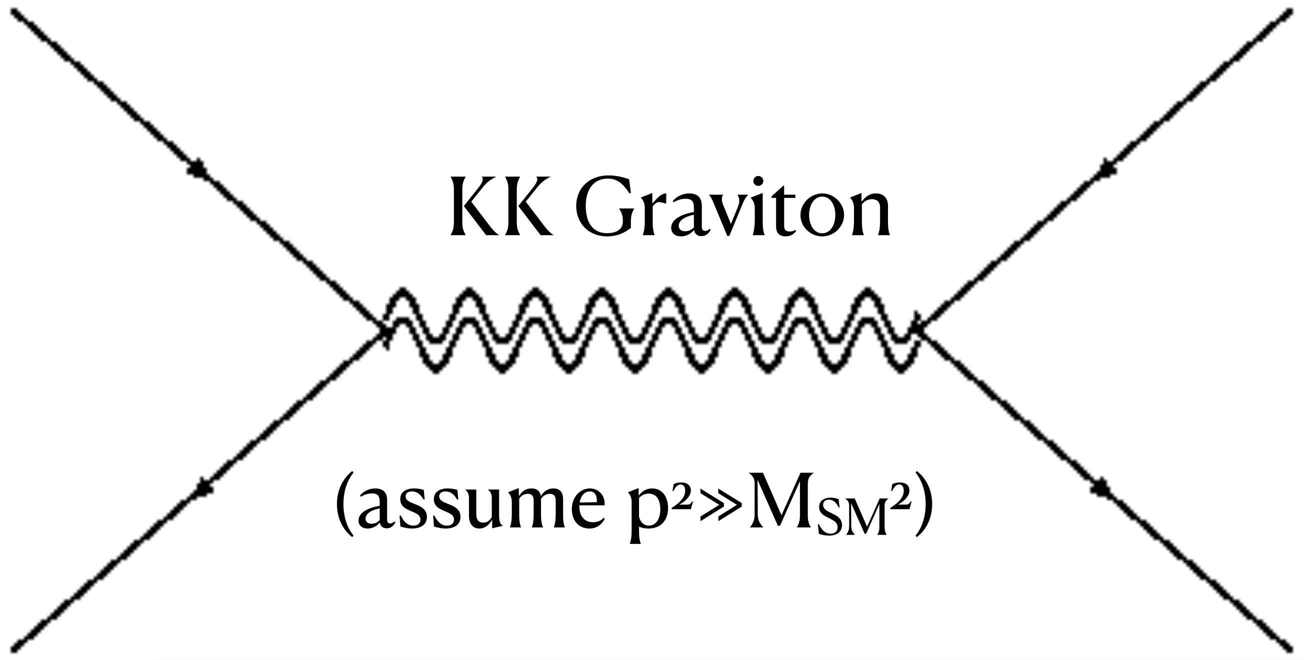

dim-6 ↓ dim-8 ↓

$$\sim 0 + \frac{p^2}{M_S^4} + \ldots$$

Han, Lykken, Zhang (1998)

$$\sigma \sim |\mathcal{M}_{SM}|^2 + \frac{1}{\Lambda^2} 2\mathrm{Re}\left[\mathcal{M}_6 \mathcal{M}_{SM}^*\right] + \frac{1}{\Lambda^4}\left\{|\mathcal{M}_6|^2 + 2\mathrm{Re}\left[\mathcal{M}_8 \mathcal{M}_{SM}^*\right]\right\}$$

Given that different UV models can lead to very different patterns between dim-6 and dim-8 coefficients, we should make as few assumptions as possible regarding their relative size in SMEFT studies, and just let the data determine their allowed range.

Searching for the SMEFT

- Searching for SMEFT-induced deviations requires a broad spectrum of experiments that probe different regions of possible parameter space. One aspect of this program is low-energy experiments, which can provide important constraints.

Example:

Cirigliano et al (2019)

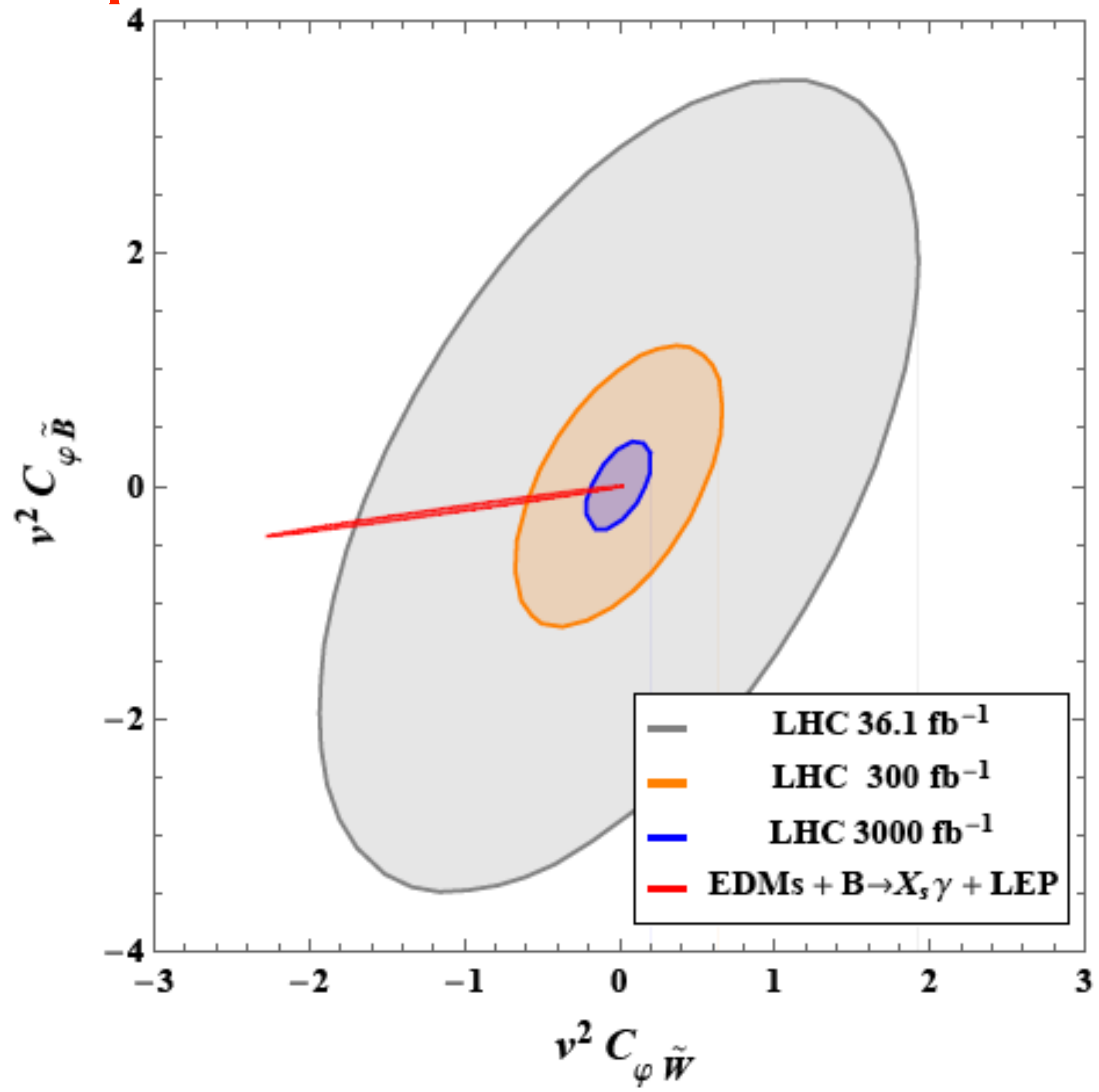

$C_{\phi\tilde{B}}$: $\phi^\dagger \phi B_{\mu\nu} \tilde{B}^{\mu\nu}$

$C_{\phi\tilde{W}}$: $\phi^\dagger \phi W_{\mu\nu} \tilde{W}^{\mu\nu}$

CP-violating gauge-Higgs interactions from low-energy observables such as EDMs complementary to high-energy LHC probes

Searching for the SMEFT

- The most natural experiments to look for SMEFT-induced deviations are high-energy ones such as the LHC, since the expansion parameter C^*E^2/Λ^2 is maximized there. Global fits to the available data are pursued by both the experimental and theoretical collaborations.

Ellis et al (2020)

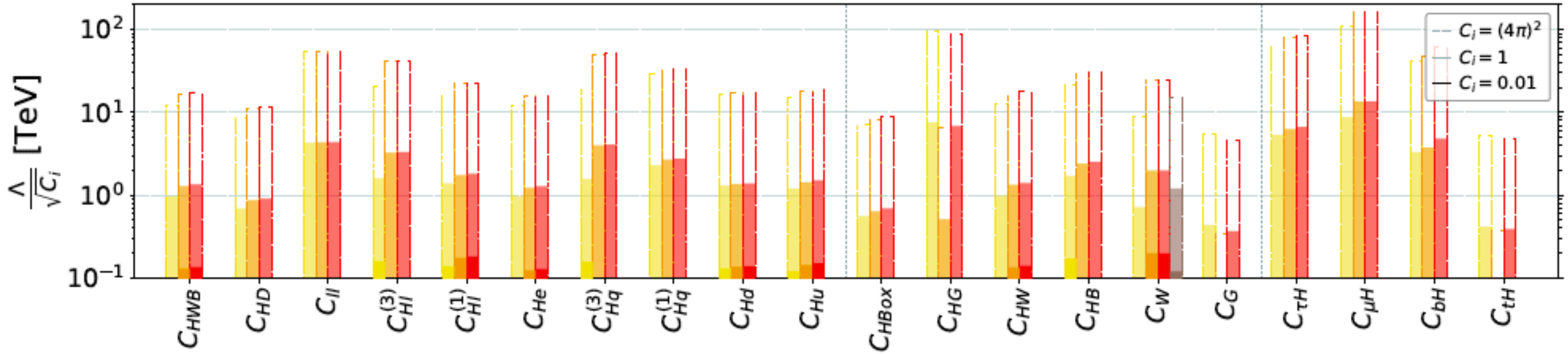

The LHC provides a rich program to search for a broad spectrum of coefficients to the TeV scale; we'll focus first on an example sector of SMEFT here

SMEFT probes at the LHC

Example: semi-leptonic four-fermion operators

- We will study in detail the LHC example of semi-leptonic four-fermion operators in the SMEFT. These are the relevant operators for the Z' versus graviton example considered before. The natural place to search for them at the LHC is through the Drell-Yan process at high energies.

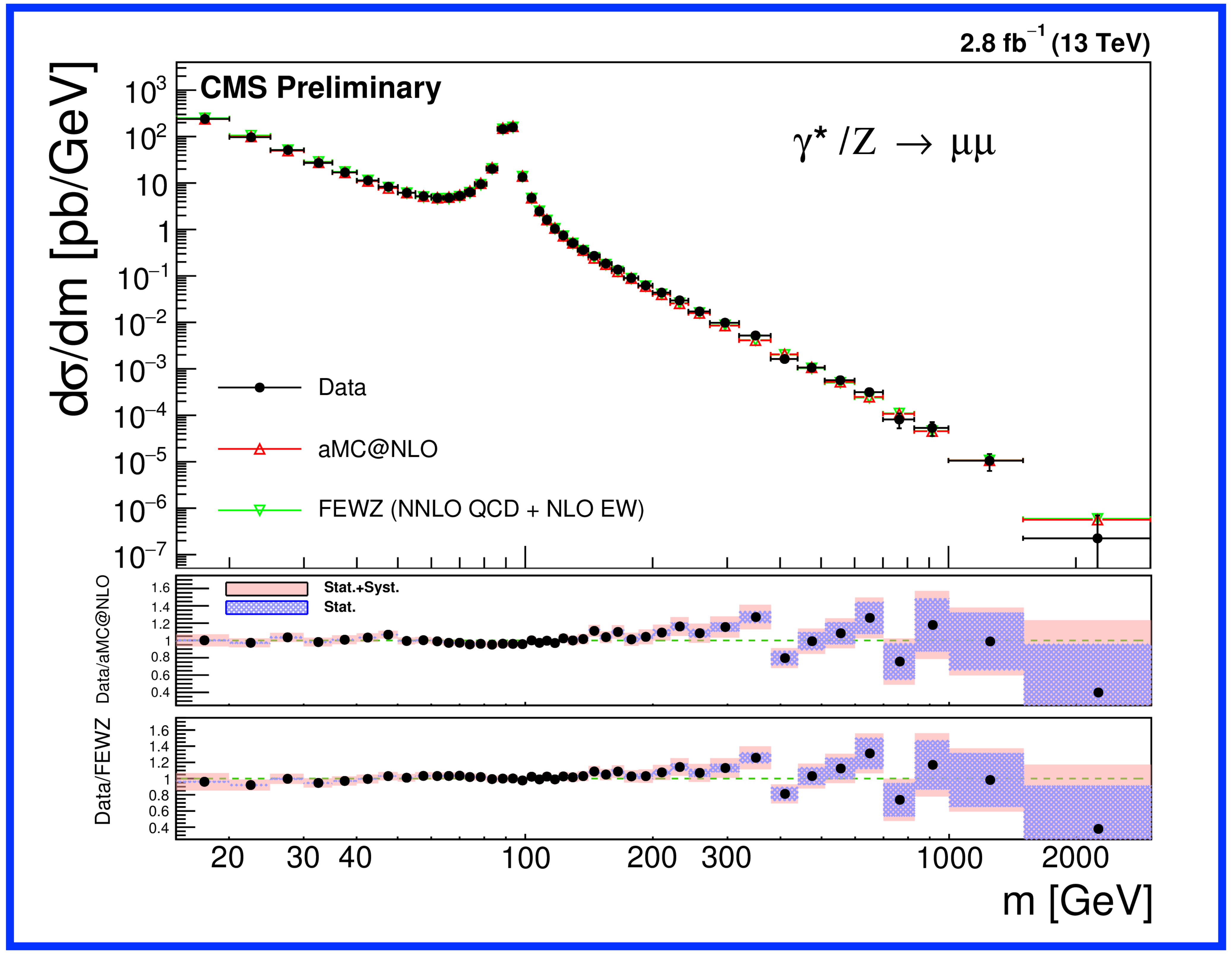

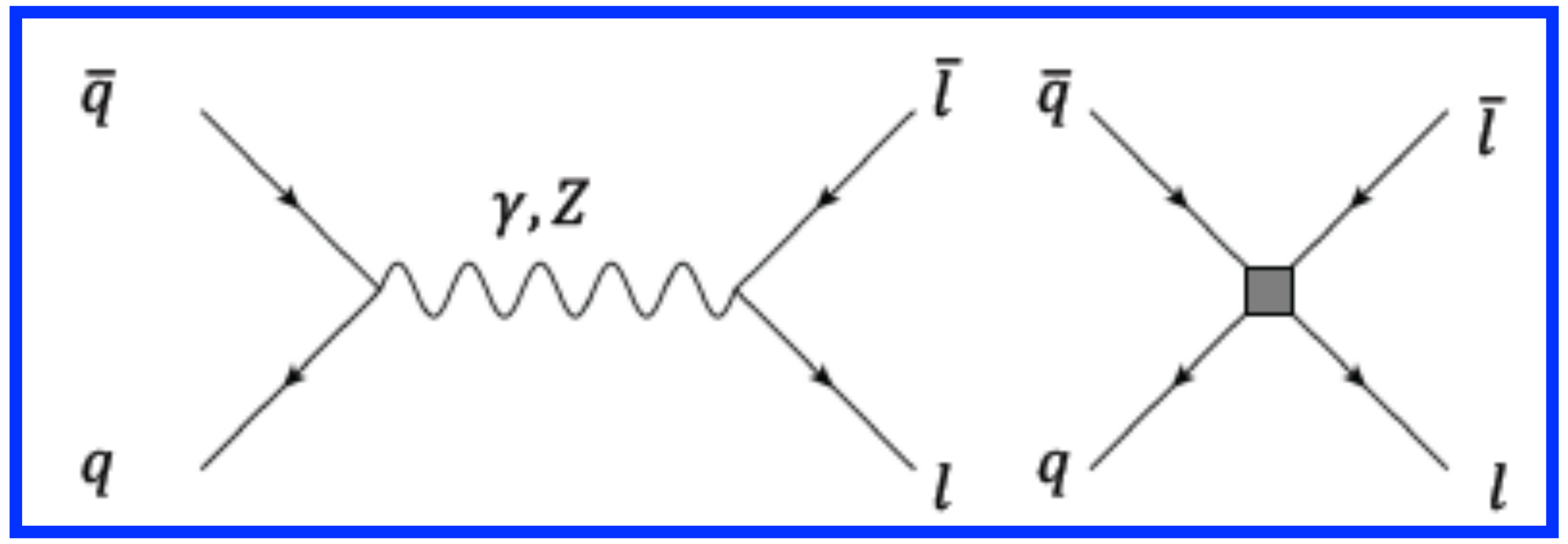

Both data and theory are precise up to high invariant masses

Operator basis

- The relevant four-fermion operators consist of seven dim-6 and 14 dim-8 operators.

Dimension 6		Dimension 8	
$\mathcal{O}_{lq}^{(1)}$	$(\bar{l}\gamma^\mu l)\,(\bar{q}\gamma_\mu q)$	$\mathcal{O}_{l^2q^2D^2}^{(1)}$	$D^\nu\,(\bar{l}\gamma^\mu l)\,D_\nu\,(\bar{q}\gamma_\mu q)$
$\mathcal{O}_{lq}^{(3)}$	$(\bar{l}\gamma^\mu\tau^i l)\,(\bar{q}\gamma_\mu\tau^i q)$	$\mathcal{O}_{l^2q^2D^2}^{(3)}$	$D^\nu\,(\bar{l}\gamma^\mu\tau^i l)\,D_\nu\,(\bar{q}\gamma_\mu\tau^i q)$
$\mathcal{O}_{eu}$	$(\bar{e}\gamma^\mu e)\,(\bar{u}\gamma_\mu u)$	$\mathcal{O}_{e^2u^2D^2}^{(1)}$	$D^\nu\,(\bar{e}\gamma^\mu e)\,D_\nu\,(\bar{u}\gamma_\mu u)$
$\mathcal{O}_{ed}$	$(\bar{e}\gamma^\mu e)\,(\bar{d}\gamma_\mu d)$	$\mathcal{O}_{e^2d^2D^2}^{(1)}$	$D^\nu\,(\bar{e}\gamma^\mu e)\,D_\nu\,(\bar{d}\gamma_\mu d)$
$\mathcal{O}_{lu}$	$(\bar{l}\gamma^\mu l)\,(\bar{u}\gamma_\mu u)$	$\mathcal{O}_{l^2u^2D^2}^{(1)}$	$D^\nu\,(\bar{l}\gamma^\mu l)\,D_\nu\,(\bar{u}\gamma_\mu u)$
$\mathcal{O}_{ld}$	$(\bar{l}\gamma^\mu l)\,(\bar{d}\gamma_\mu d)$	$\mathcal{O}_{l^2d^2D^2}^{(1)}$	$D^\nu\,(\bar{l}\gamma^\mu l)\,D_\nu\,(\bar{d}\gamma_\mu d)$
$\mathcal{O}_{qe}$	$(\bar{q}\gamma^\mu q)\,(\bar{e}\gamma_\mu e)$	$\mathcal{O}_{q^2e^2D^2}^{(1)}$	$D^\nu\,(\bar{q}\gamma^\mu q)\,D_\nu\,(\bar{e}\gamma_\mu e)$

Dimension 8

$$\mathcal{O}_{8,ed\partial 2} = (\bar{e}\gamma_\mu \overleftrightarrow{D}_\nu e)(\bar{d}\gamma^\mu \overleftrightarrow{D}^\nu d),$$
$$\mathcal{O}_{8,eu\partial 2} = (\bar{e}\gamma_\mu \overleftrightarrow{D}_\nu e)(\bar{u}\gamma^\mu \overleftrightarrow{D}^\nu u),$$
$$\mathcal{O}_{8,ld\partial 2} = (\bar{l}\gamma_\mu \overleftrightarrow{D}_\nu l)(\bar{d}\gamma^\mu \overleftrightarrow{D}^\nu d),$$
$$\mathcal{O}_{8,lu\partial 2} = (\bar{l}\gamma_\mu \overleftrightarrow{D}_\nu l)(\bar{u}\gamma^\mu \overleftrightarrow{D}^\nu u),$$
$$\mathcal{O}_{8,qe\partial 2} = (\bar{e}\gamma_\mu \overleftrightarrow{D}_\nu e)(\bar{q}\gamma^\mu \overleftrightarrow{D}^\nu q).$$
$$\mathcal{O}_{8,lq\partial 3} = (\bar{l}\gamma_\mu \overleftrightarrow{D}_\nu l)(\bar{q}\gamma^\mu \overleftrightarrow{D}^\nu q),$$
$$\mathcal{O}_{8,lq\partial 4} = (\bar{l}\tau^I\gamma_\mu \overleftrightarrow{D}_\nu l)(\bar{q}\tau^I\gamma^\mu \overleftrightarrow{D}^\nu q)$$

Relevant operators for our analysis; note q,l are left-handed doublets; e,u,d are right-handed singlets

Operator basis

- The relevant four-fermion operators consist of seven dim-6 and 14 dim-8 operators.

$$O_{\varphi\ell}^{(1)} = (\varphi^\dagger i \overleftrightarrow{D}_\mu \varphi)(\bar{\ell}\gamma^\mu \ell)$$
$$O_{\varphi\ell}^{(3)} = (\varphi^\dagger i \overleftrightarrow{D}_\mu \tau^I \varphi)(\bar{\ell}\gamma^\mu \tau^I \ell)$$
$$O_{\varphi e} = (\varphi^\dagger i \overleftrightarrow{D}_\mu \varphi)(\bar{e}\gamma^\mu e)$$
$$O_{\varphi q}^{(1)} = (\varphi^\dagger i \overleftrightarrow{D}_\mu \varphi)(\bar{q}\gamma^\mu q)$$
$$O_{\varphi q}^{(3)} = (\varphi^\dagger i \overleftrightarrow{D}_\mu \tau^I \varphi)(\bar{q}\gamma^\mu \tau^I q)$$
$$O_{\varphi u} = (\varphi^\dagger i \overleftrightarrow{D}_\mu \varphi)(\bar{u}\gamma^\mu u)$$
$$O_{\varphi d} = (\varphi^\dagger i \overleftrightarrow{D}_\mu \varphi)(\bar{d}\gamma^\mu d)$$

Dawson, Giardino (2019)

C_k	95% CL, $\Lambda = 1$ TeV
$C_{\varphi\ell}^{(1)}$	$[-0.043, 0.012]$
$C_{\varphi\ell}^{(3)}$	$[-0.012, 0.0029]$
$C_{\varphi e}$	$[-0.013, 0.0094]$
$C_{\varphi q}^{(1)}$	$[-0.027, 0.043]$
$C_{\varphi q}^{(3)}$	$[-0.011, 0.014]$
$C_{\varphi u}$	$[-0.072, 0.091]$
$C_{\varphi d}$	$[-0.16, 0.060]$
$C_{\varphi WB}$	$[-0.0088, 0.0013]$

Other operators contribute as well, and shift the ffV vertices

These are better constrained by the precision Z-pole data of LEP, SLC; however, these experiments only weakly constrain four-fermion operators

Lepton angular distributions

- Begin with the second column of dimension-8 operators; the derivative structure leads to l=3 spherical harmonics in the differential cross section. Cannot get this structure from dimension-6 in the SMEFT, nor from the SM to all orders in QCD. Only weakly generated by EW corrections, specifically angular-dependent NLL Sudakov logarithms

Dimension 8

$$\begin{aligned}
\mathcal{O}_{8,ed\partial 2} &= (\bar{e}\gamma_\mu \overleftrightarrow{D}_\nu e)(\bar{d}\gamma^\mu \overleftrightarrow{D}^\nu d), \\
\mathcal{O}_{8,eu\partial 2} &= (\bar{e}\gamma_\mu \overleftrightarrow{D}_\nu e)(\bar{u}\gamma^\mu \overleftrightarrow{D}^\nu u), \\
\mathcal{O}_{8,ld\partial 2} &= (\bar{l}\gamma_\mu \overleftrightarrow{D}_\nu l)(\bar{d}\gamma^\mu \overleftrightarrow{D}^\nu d), \\
\mathcal{O}_{8,lu\partial 2} &= (\bar{l}\gamma_\mu \overleftrightarrow{D}_\nu l)(\bar{u}\gamma^\mu \overleftrightarrow{D}^\nu u), \\
\mathcal{O}_{8,qe\partial 2} &= (\bar{e}\gamma_\mu \overleftrightarrow{D}_\nu e)(\bar{q}\gamma^\mu \overleftrightarrow{D}^\nu q). \\
\mathcal{O}_{8,lq\partial 3} &= (\bar{l}\gamma_\mu \overleftrightarrow{D}_\nu l)(\bar{q}\gamma^\mu \overleftrightarrow{D}^\nu q), \\
\mathcal{O}_{8,lq\partial 4} &= (\bar{l}\tau^I\gamma_\mu \overleftrightarrow{D}_\nu l)(\bar{q}\tau^I\gamma^\mu \overleftrightarrow{D}^\nu q)
\end{aligned}$$

Drell-Yan angular distributions:

Alioli, RB, Mereghetti, Petriello (2020)

$$\begin{aligned}
\frac{d\sigma}{dm_{ll}^2 dy d\Omega_l} = \frac{3}{16\pi}\frac{d\sigma}{dm_{ll}^2 dy}\Big\{&(1+c_\theta^2) + \frac{A_0}{2}(1-3c_\theta^2) \\
&+A_1 s_{2\theta}c_\phi + \frac{A_2}{2}s_\theta^2 c_{2\phi} + A_3 s_\theta c_\phi + A_4 c_\theta \\
&+A_5 s_\theta^2 s_{2\phi} + A_6 s_{2\theta}s_\phi + A_7 s_\theta s_\phi \\
&+B_3^e s_\theta^3 c_\phi + B_3^o s_\theta^3 s_\phi + B_2^e s_\theta^2 c_\theta c_{2\phi} \\
&+B_2^o s_\theta^2 c_\theta s_{2\phi} + \frac{B_1^e}{2}s_\theta(5c_\theta^2-1)c_\phi \\
&+\frac{B_1^o}{2}s_\theta(5c_\theta^2-1)s_\phi + \frac{B_0}{2}(5c_\theta^3-3c_\theta)\Big\}
\end{aligned}$$

- The B_i account for the potential l=3 angular behavior at dim-8
- $B_{1\text{-}3}$ first generated at $O(\alpha_s/\Lambda^4)$
- Focus on B_0, which is generated at $O(1/\Lambda^4)$

LHC reach with angular analysis

Alioli, RB, Mereghetti, Petriello (2020)

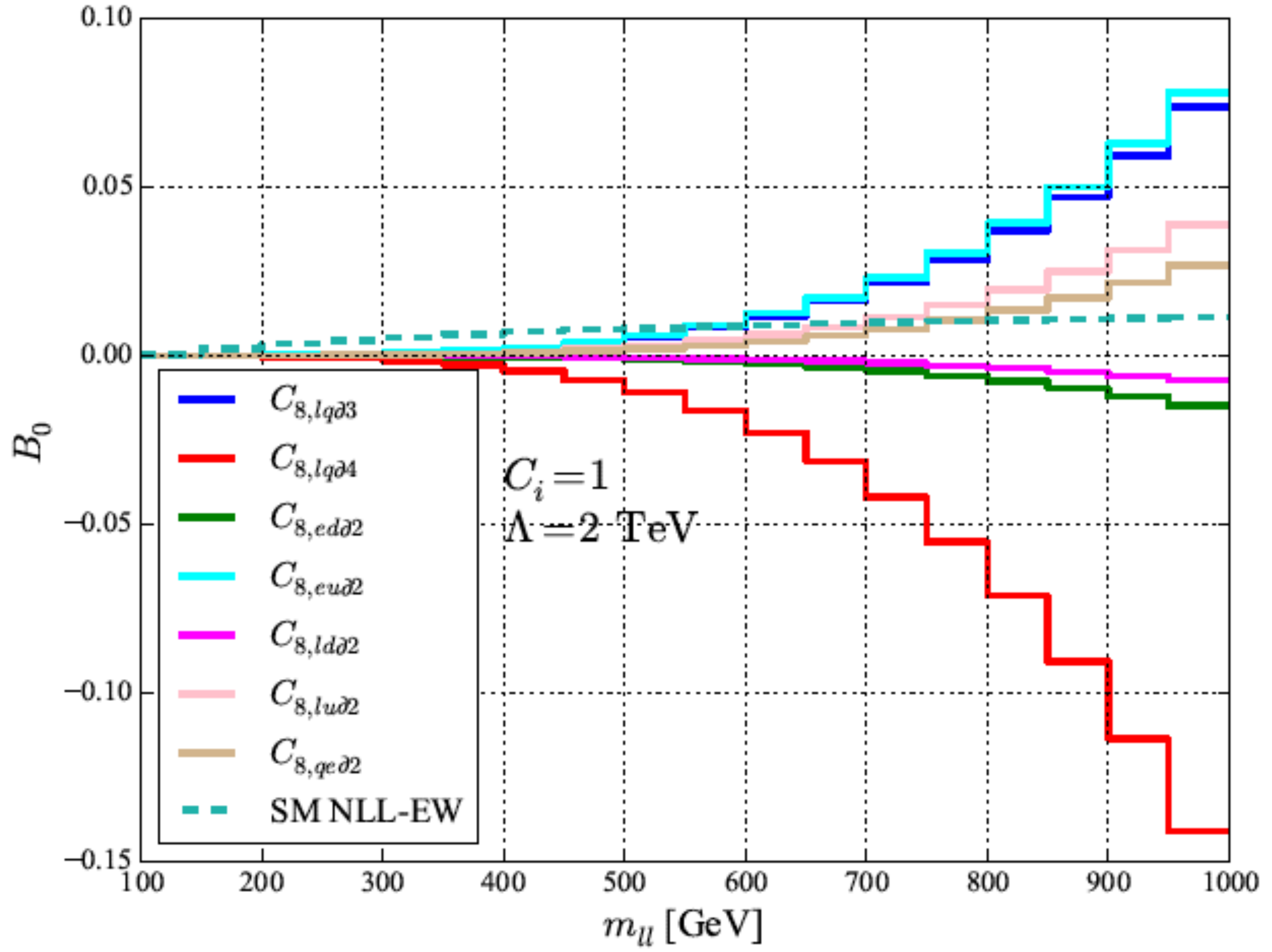

- Turn on each operator separately, set UV scale Λ=2 TeV
- Several operators lead to significant deviations from SM predictions

LHC reach with angular analysis

Alioli, RB, Mereghetti, Petriello (2020)

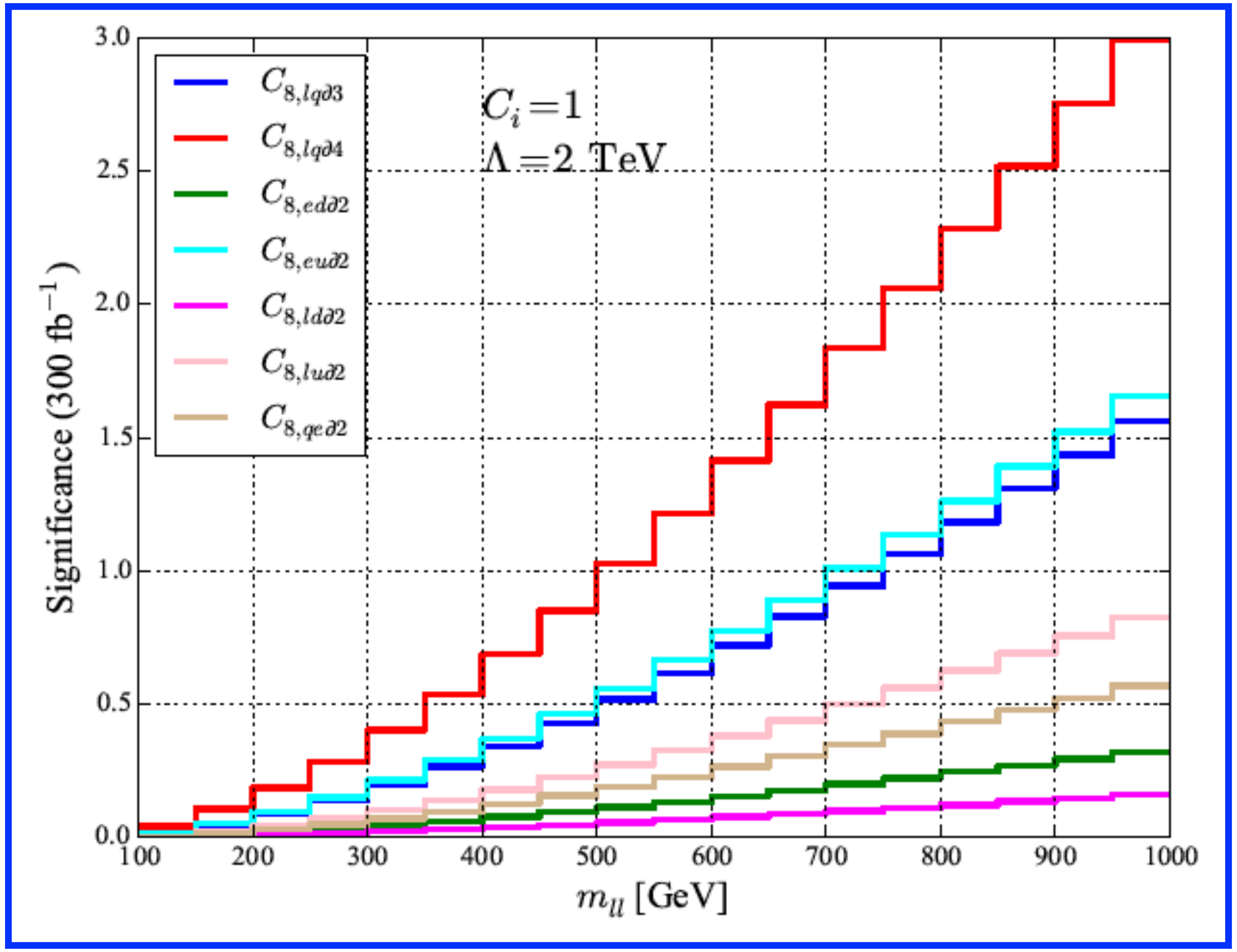

- Single-bin significance reaches 3 for largest operator with 300 fb^{-1}
- Combining 600-1000 GeV bins leads to Sig>6 for largest operator, Sig>3.5 for next two
- HL-LHC increases these results by √10
- We have discovery potential at the LHC for some of these coefficients!

Promising "smoking gun" signature of dim-8 at the LHC, but need a dedicated angular analysis which doesn't yet exist!

Invariant mass and A_{FB} constraints

- We now turn our attention to constraints from existing data sets: invariant mass distributions and forward-backward asymmetries. These are sensitive to the set of operators not probed by the previous angular analysis.

No.	Experiment	$\sqrt{s}$	Measurement	Luminosity	m_{ll}^{low}	Ref.
I	ATLAS	8 TeV	$d\sigma/dm$	20.3 fb^{-1}	116-1000 GeV	[24]
II	CMS	13 TeV	$d\sigma/dm$	137 fb^{-1} (ee) 140 fb^{-1} $(\mu\mu)$	200-2210 GeV (ee) 210-2290 GeV $(\mu\mu)$	[25]
III	CMS	8 TeV	A_{FB}^{*}	19.7 fb^{-1}	120-500 GeV	[26]
IV	CMS	13 TeV	A_{FB}	138 fb^{-1}	170-1000 GeV	[27]

Excellent test case for how well LHC covers the SMEFT; significant high-luminosity, high-quality data

Single parameter vs. marginalized fits

- We begin with a fit to the linear dimension-6 SMEFT basis. There are seven relevant semi-leptonic four-fermion Wilson coefficients with this assumption. We first consider single-parameter versus marginalized fits

RB, Huang, Petriello (2023)

Dimension 6	
$\mathcal{O}_{lq}^{(1)}$	$(\bar{l}\gamma^\mu l)(\bar{q}\gamma_\mu q)$
$\mathcal{O}_{lq}^{(3)}$	$(\bar{l}\gamma^\mu \tau^i l)(\bar{q}\gamma_\mu \tau^i q)$
$\mathcal{O}_{eu}$	$(\bar{e}\gamma^\mu e)(\bar{u}\gamma_\mu u)$
$\mathcal{O}_{ed}$	$(\bar{e}\gamma^\mu e)(\bar{d}\gamma_\mu d)$
$\mathcal{O}_{lu}$	$(\bar{l}\gamma^\mu l)(\bar{u}\gamma_\mu u)$
$\mathcal{O}_{ld}$	$(\bar{l}\gamma^\mu l)(\bar{d}\gamma_\mu d)$
$\mathcal{O}_{qe}$	$(\bar{q}\gamma^\mu q)(\bar{e}\gamma_\mu e)$

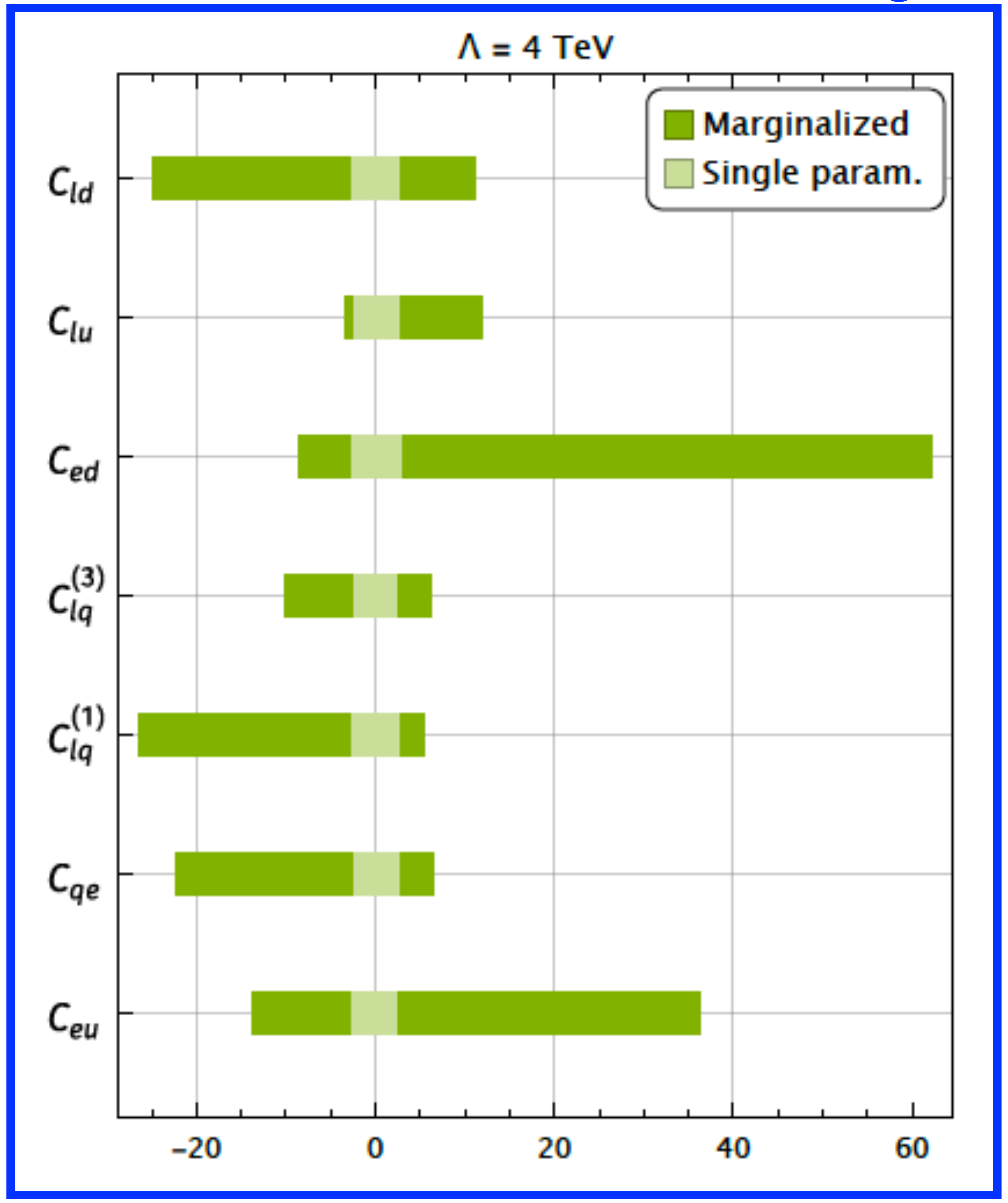

There is a significant difference between the single-parameter and marginalized fits, indicating the need to turn all Wilson coefficients on simultaneously

Linear vs. quadratic fits

- We now consider the difference between expanding the dimension-6 SMEFT corrections to both linear and quadratic orders. As an example we will turn on two coefficients only.

RB, Huang, Petriello (2023)

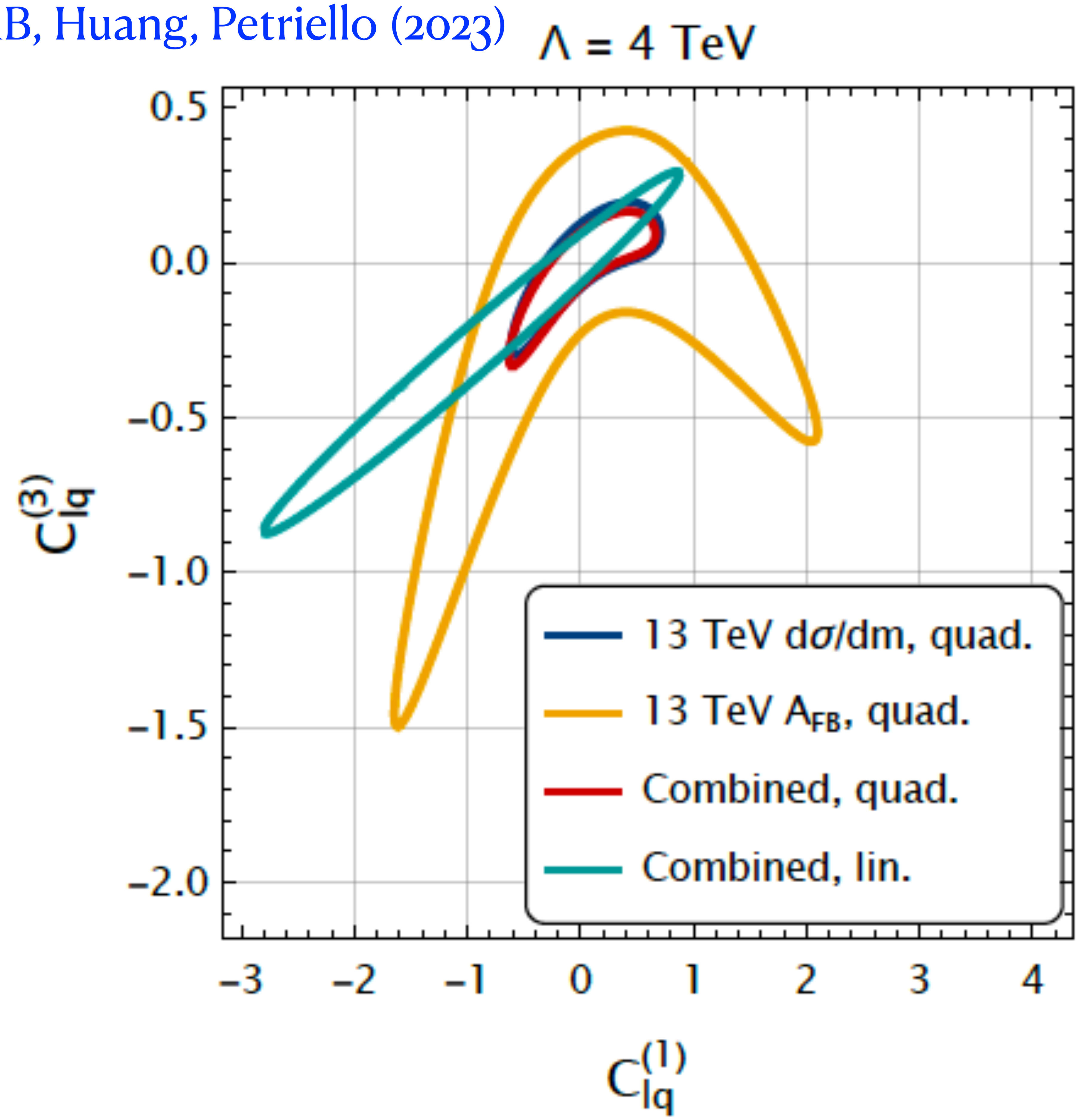

- The A_{FB} data set (boomerang shape) alone exhibits significant degeneracies; need to fit to multiple data sets!
- Linear (cyan) and quadratic (red) combined fits differ significantly; important to include higher-order terms in the SMEFT expansion!
- Note that A_{FB} data doesn't improve the combined fit; the power comes from the invariant mass data

Dimension-8 effects

- If quadratic dimension-6 terms have an effect, dimension-8 terms should as well.

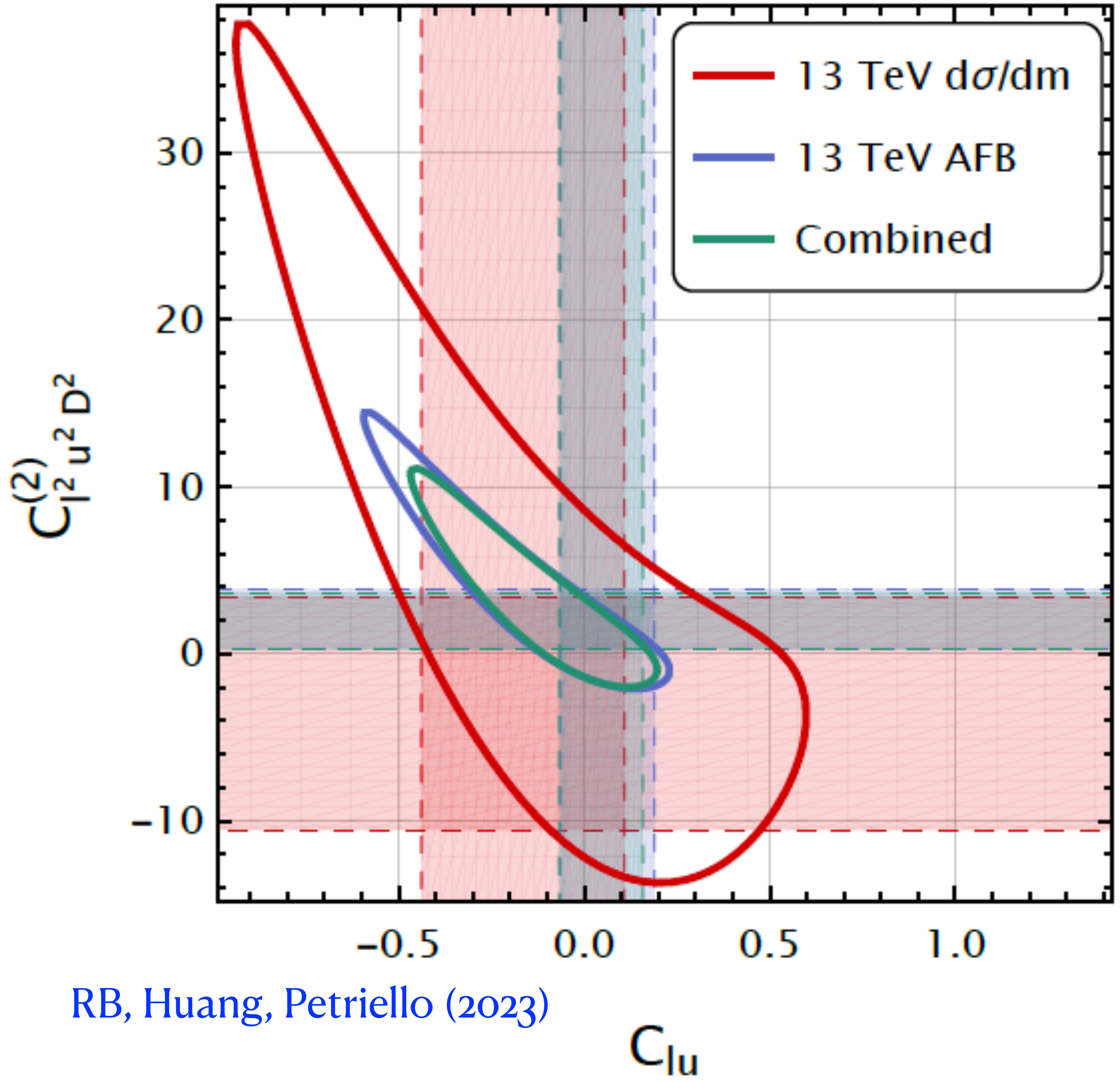

RB, Huang, Petriello (2023)

- Turn on left-handed lepton coupling to right handed up quark at dim-6 and dim-8 as an example.
- Shaded regions are the one-parameter constraints at 95% CL. Ellipses are when both parameters are turned on.
- Significant shifts! For example, the allowed region of C_{lu} extends to -0.6 with dim-8 turned on; in the single parameter fit it extends only to -0.1.
- Note this time constraints primarily from A_{FB}!

This is with all the relevant LHC DY data!

What have we learned so far?

- Single-parameter fits give bounds significantly different than those obtained from a full fit.
- The use of all available data is needed to help reduce degeneracies in the parameter space.
- Quadratic dimension-6 terms can have an important impact on SMEFT fits.
- Dimension-8 terms, which appear at the same order in the SMEFT expansion as quadratic dimension-6, not surprisingly have an important effect in fits.

The LHC alone isn't enough to fully cover the parameter space, degeneracies exist between dim6 coefficients themselves and between dim6 and dim8.

Future DIS experiments

- Another possibility of probing the SMEFT parameter space is with future DIS experiments. A host of facilities spanning low and high energies are planned for both the near and far future.

High energy DIS:

- Electron-Ion Collider (EIC): $\sqrt{s}$~140 GeV
- Future Circular Collider (FCC-eh): $\sqrt{s}$~3.4 TeV
- Large Hadron Electron Collider (LHeC): $\sqrt{s}$~1.3 TeV

Low energy PVES:

- Solenoidal Large Inensity Device (SoLID) at Jlab
- P2 at Mainz

Sensitive to the same operators as the Drell-Yan process at the LHC

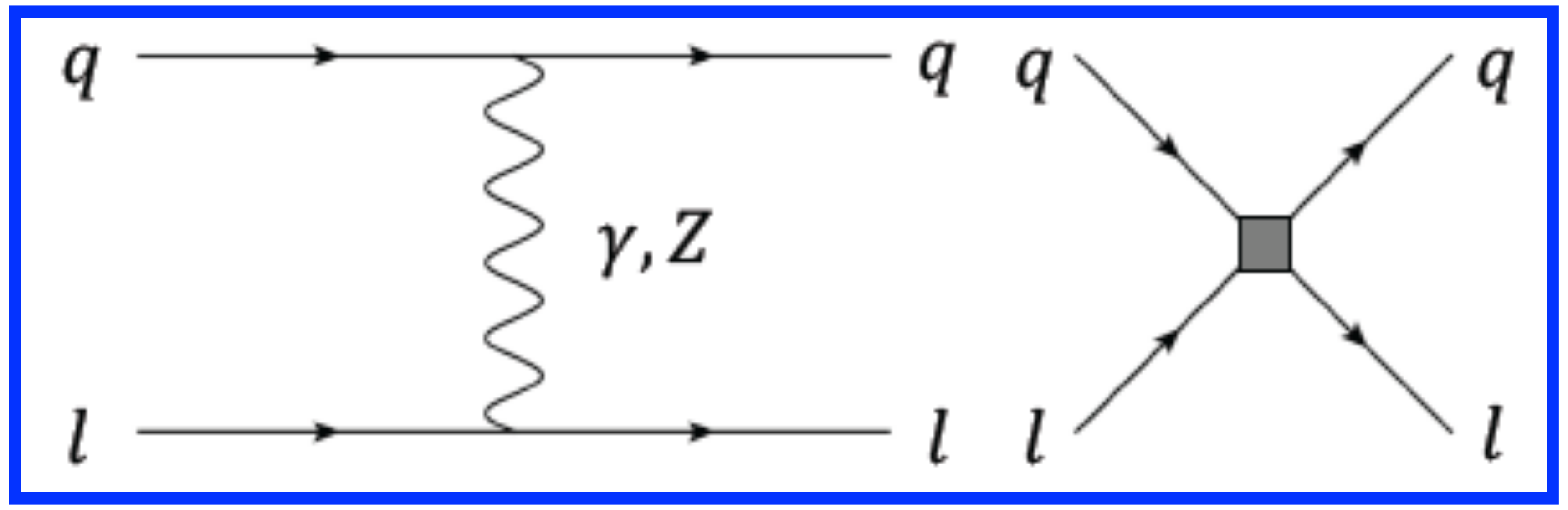

Future DIS experiments

- Another possibility of probing the SMEFT parameter space is with future DIS experiments. A host of facilities spanning low and high energies are planned for both the near and far future.

High energy DIS:

- Electron-Ion Collider (EIC): √s~140 GeV
- Future Circular Collider (FCC-eh): √s~3.4 TeV
- Large Hadron Electron Collider (LHeC): √s~1.3 TeV

Low energy PVES:

- Solenoidal Large Inensity Device (SoLID) at Jlab
- P2 at Mainz

A key feature shared by all of these experiments is the ability to polarize beams; a key distinction from the LHC!

$$\frac{d^2\sigma_u^{\gamma SMEFT}}{dx dQ^2} = -x\frac{Q_u Q^2}{8\pi\alpha}\Big[C_{eu}(1+\lambda_u)(1+\lambda_e) + (C_{lq}^{(1)} - C_{lq}^{(3)})(1-\lambda_u)(1-\lambda_e) + (1-y)^2 C_{lu}(1+\lambda_u)(1-\lambda_e) + (1-y)^2 C_{qe}(1-\lambda_u)(1+\lambda_e)\Big]$$

Disentangle Wilson coefficients with polarization

SMEFT probes at the EIC

Key features of the EIC

- The EIC will be constructed at BNL in the coming decade. In our analysis of SMEFT at the EIC we assume the following run parameters.

Deuteron beam: Proton beam:

D1	5 GeV $\times$ 41 GeV eD, 4.4 fb^{-1}	P1	5 GeV $\times$ 41 GeV ep, 4.4 fb^{-1}
D2	5 GeV $\times$ 100 GeV eD, 36.8 fb^{-1}	P2	5 GeV $\times$ 100 GeV ep, 36.8 fb^{-1}
D3	10 GeV $\times$ 100 GeV eD, 44.8 fb^{-1}	P3	10 GeV $\times$ 100 GeV ep, 44.8 fb^{-1}
D4	10 GeV $\times$ 137 GeV eD, 100 fb^{-1}	P4	10 GeV $\times$ 275 GeV ep, 100 fb^{-1}
D5	18 GeV $\times$ 137 GeV eD, 15.4 fb^{-1}	P5	18 GeV $\times$ 275 GeV ep, 15.4 fb^{-1}
		P6	18 GeV $\times$ 275 GeV ep, 100 fb^{-1}

Additionally assume 70% hadron beam polarization, 80% electron beam polarization

- Allows us to study the interplay between high energy/low luminosity (for example, P5) versus low energy/high luminosity (for example, P4).
- Polarized deuteron and proton copies of these data sets are also studied, and labeled as ΔD, ΔP.
- Data sets where the lepton charge asymmetry is considered are labeled as LD, LP.

Observables at the EIC

- The ability to polarize both beams at the EIC, and potentially swap an electron beam for a positron beam, leads to a host of observables.
  - Polarized electrons, unpolarized hadrons: $$A_{\mathrm{PV}} = \frac{\mathrm{d}\sigma_\ell}{\mathrm{d}\sigma_0}$$
  - Unpolarized electrons, polarized hadrons: $$\Delta A_{\mathrm{PV}} = \frac{\mathrm{d}\sigma_H}{\mathrm{d}\sigma_0}$$
  - Lepton charge asymmetries: $$A_{\mathrm{LC}} = \frac{\mathrm{d}\sigma_0(e^+H) - \mathrm{d}\sigma_0(e^-H)}{\mathrm{d}\sigma_0(e^+H) + \mathrm{d}\sigma_0(e^-H)}$$

Observables at the EIC

- The ability to polarize both beams at the EIC, and potentially swap an electron beam for a positron beam, leads to a host of observables.
  - Polarized electrons, unpolarized hadrons: $A_{\mathrm{PV}} = \frac{d\sigma_\ell}{d\sigma_0}$
  - Unpolarized electrons, polarized hadrons: $\Delta A_{\mathrm{PV}} = \frac{d\sigma_H}{d\sigma_0}$
  - Lepton charge asymmetries: $A_{\mathrm{LC}} = \frac{d\sigma_0(e^+H) - d\sigma_0(e^-H)}{d\sigma_0(e^+H) + d\sigma_0(e^-H)}$

$$d\sigma_0 = \frac{1}{4}\sum_q f_{q/H}[d\sigma^{++} + d\sigma^{+-} + d\sigma^{-+} + d\sigma^{--}] : \text{unpol. } \ell + \text{unpol. } H$$

$$d\sigma_\ell = \frac{1}{4}\sum_q f_{q/H}[d\sigma^{++} + d\sigma^{+-} - d\sigma^{-+} - d\sigma^{--}] : \text{pol. } \ell + \text{unpol. } H$$

$$d\sigma_H = \frac{1}{4}\sum_q \Delta f_{q/H}[d\sigma^{++} - d\sigma^{+-} + d\sigma^{-+} - d\sigma^{--}] : \text{unpol. } \ell + \text{pol. } H$$

Observables at the EIC

- The ability to polarize both beams at the EIC, and potentially swap an electron beam for a positron beam, leads to a host of observables.

  - Polarized electrons, unpolarized hadrons: $$A_{\rm PV} = \frac{d\sigma_\ell}{d\sigma_0}$$
  - Unpolarized electrons, polarized hadrons: $$\Delta A_{\rm PV} = \frac{d\sigma_H}{d\sigma_0}$$
  - Lepton charge asymmetries: $$A_{\rm LC} = \frac{d\sigma_0(e^+H) - d\sigma_0(e^-H)}{d\sigma_0(e^+H) + d\sigma_0(e^-H)}$$

Simulation details:

- Smearing, bin migration accounted for
- Inelasticity cuts: y>0.1, y<0.9
- x<0.5, Q>10 GeV to avoid uncertainties from non-perturbative QCD and nuclear dynamics

Error budget example: unpolarized protons

- As an example of the expected EIC errors we will study the error budget for P5, the unpolarized high-energy proton scenario.
- Bins first ordered in Q^2. Within each Q^2 bin we then order in x; HL is a proposed high-luminosity option with an increase by a factor of 10 w.r.t the nominal integrated luminosity

RB et al (2022)

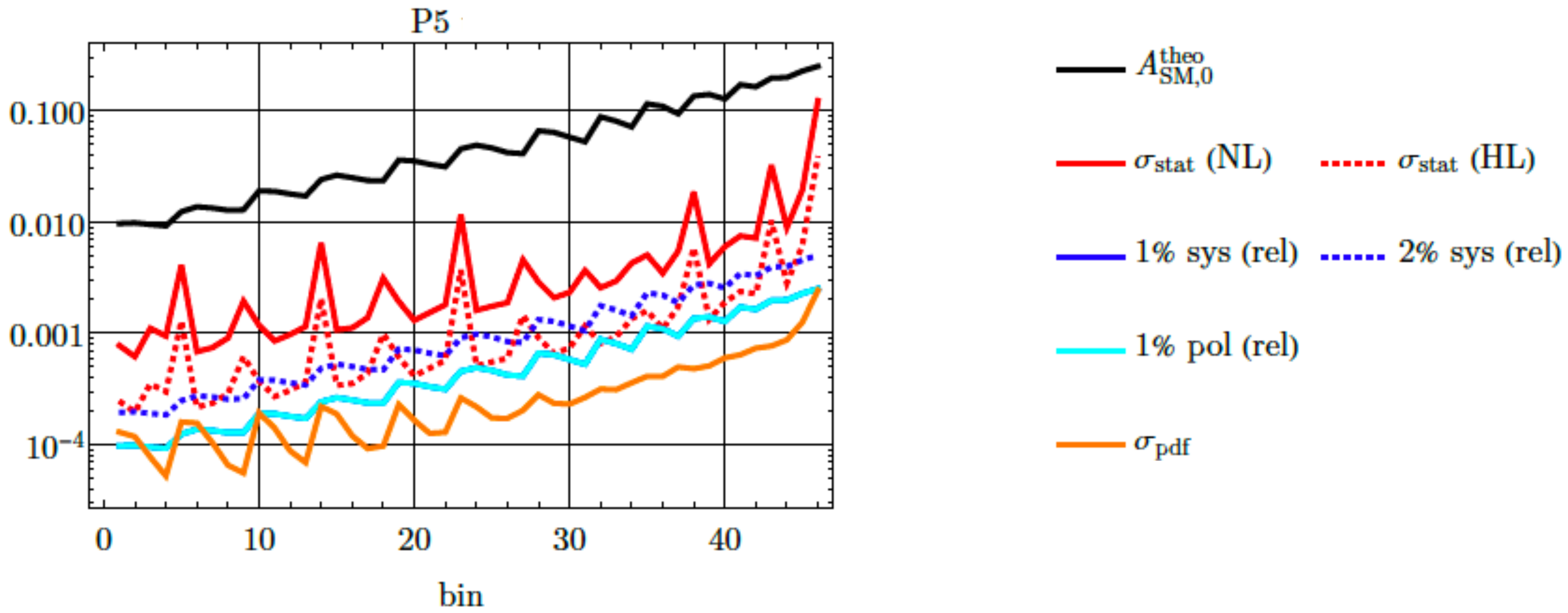

Statistical uncertainties dominant with nominal luminosity; systematic errors more relevant at high luminosity; PDF errors negligible. **Asymmetry much larger than all uncertainties.**

Single-parameter fits

- We will first consider the single-parameter fits, to understand the scales that can be probed at and EIC.

Note: lighter histograms obtained by fitting polarization uncertainty as a nuisance parameter in the fit; results in stronger constraints for polarized lepton cases

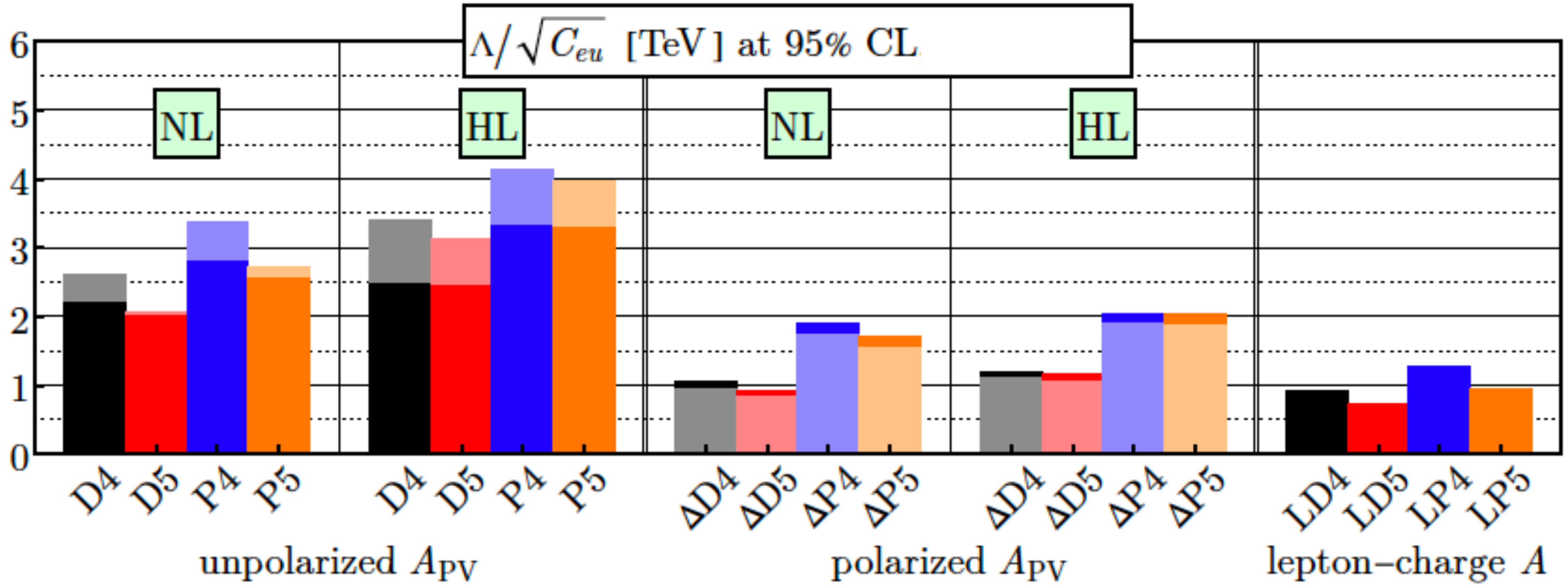

Trends:

- Proton sensitivities stronger than deuteron ones
- Unpolarized hadrons, polarized electrons offer strongest probes
- Lepton-charge asymmetries provide weakest probes

Single-parameter fits

- We will first consider the single-parameter fits, to understand the scales that can be probed at and EIC.

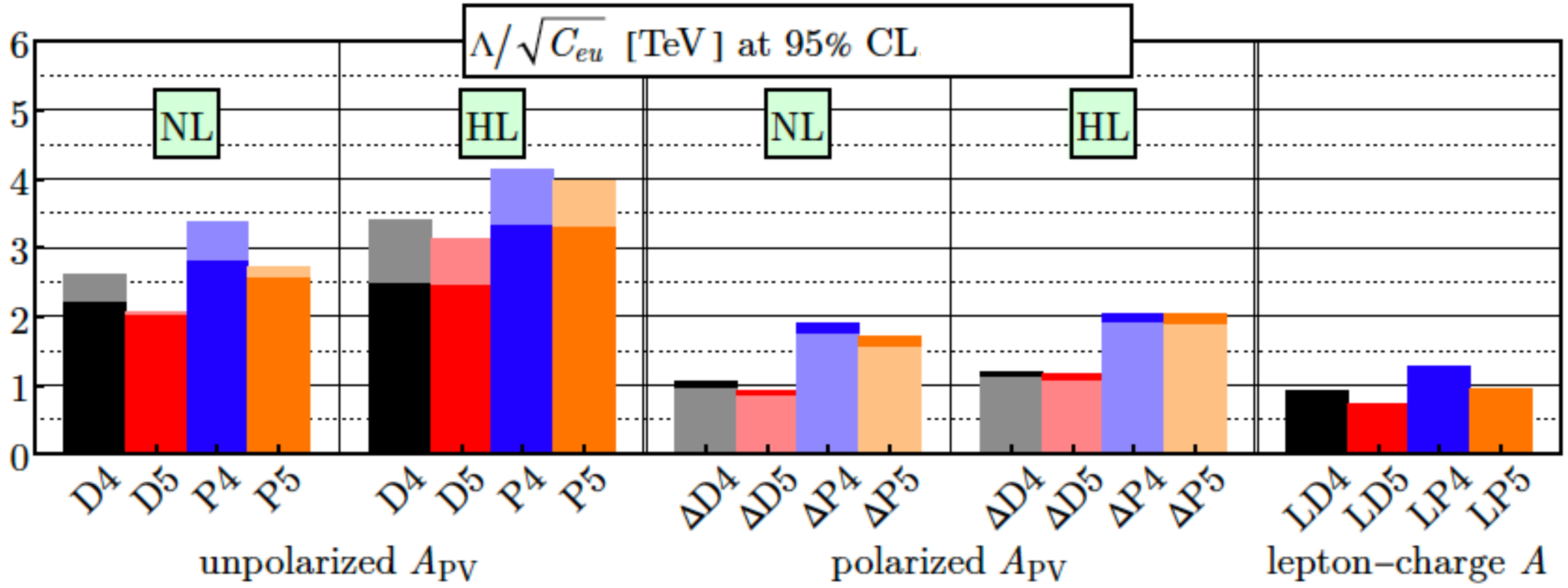

3 TeV scales probes with nominal luminosity, 4 TeV with high luminosity. Competitive with current LHC bounds.

Single-parameter fits

- We will first consider the single-parameter fits, to understand the scales that can be probed at and EIC.

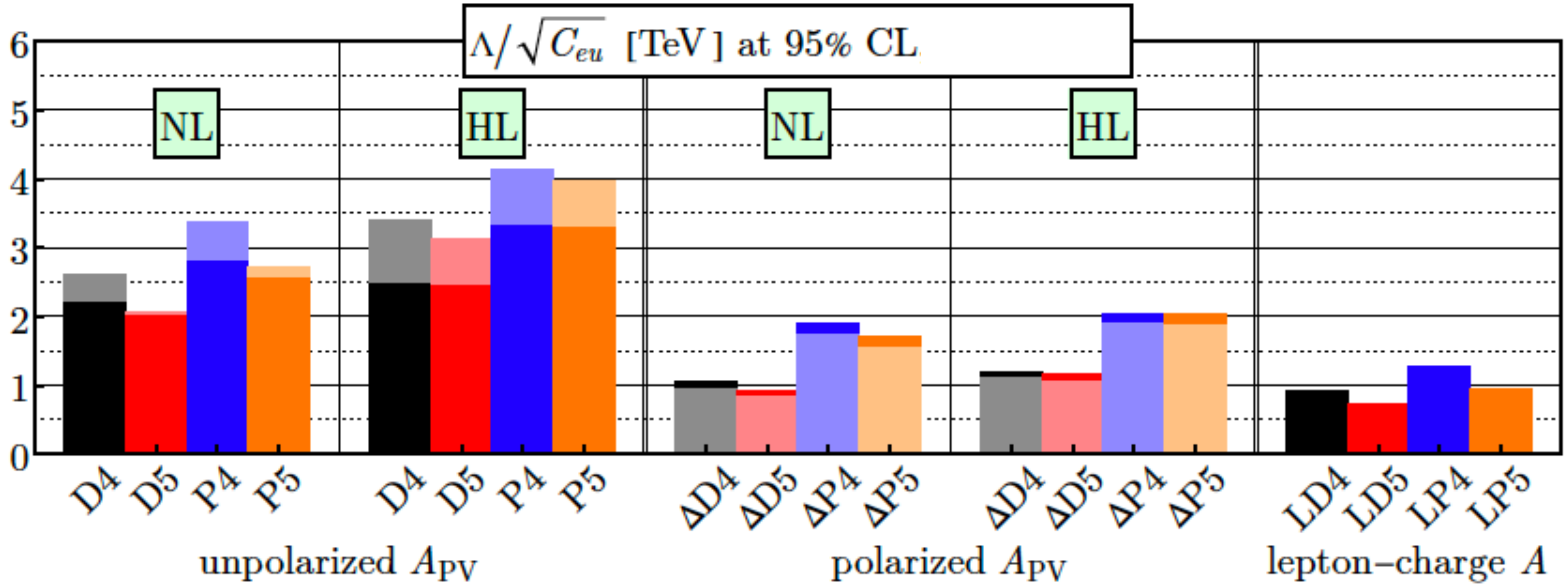

We have performed this study at dimension-6. Note that the $\Lambda/\sqrt{C}$ bounds are much greater than the momentum transfer $Q<50$ GeV. The expansion parameter $CQ^2/\Lambda^2 << 1$ unlike at the LHC, indicating that dim-8 is very suppressed. We will revisit dim-8 in DIS later!

Multi-parameter fits

- We can turn on more Wilson coefficients to test for degeneracies and check for degradation of the bounds. Only slightly weaker bounds in a 6-dimensional fit. The EIC can probe the full parameter space of semi-leptonic four-fermion Wilson coefficients.

RB et al (2022)

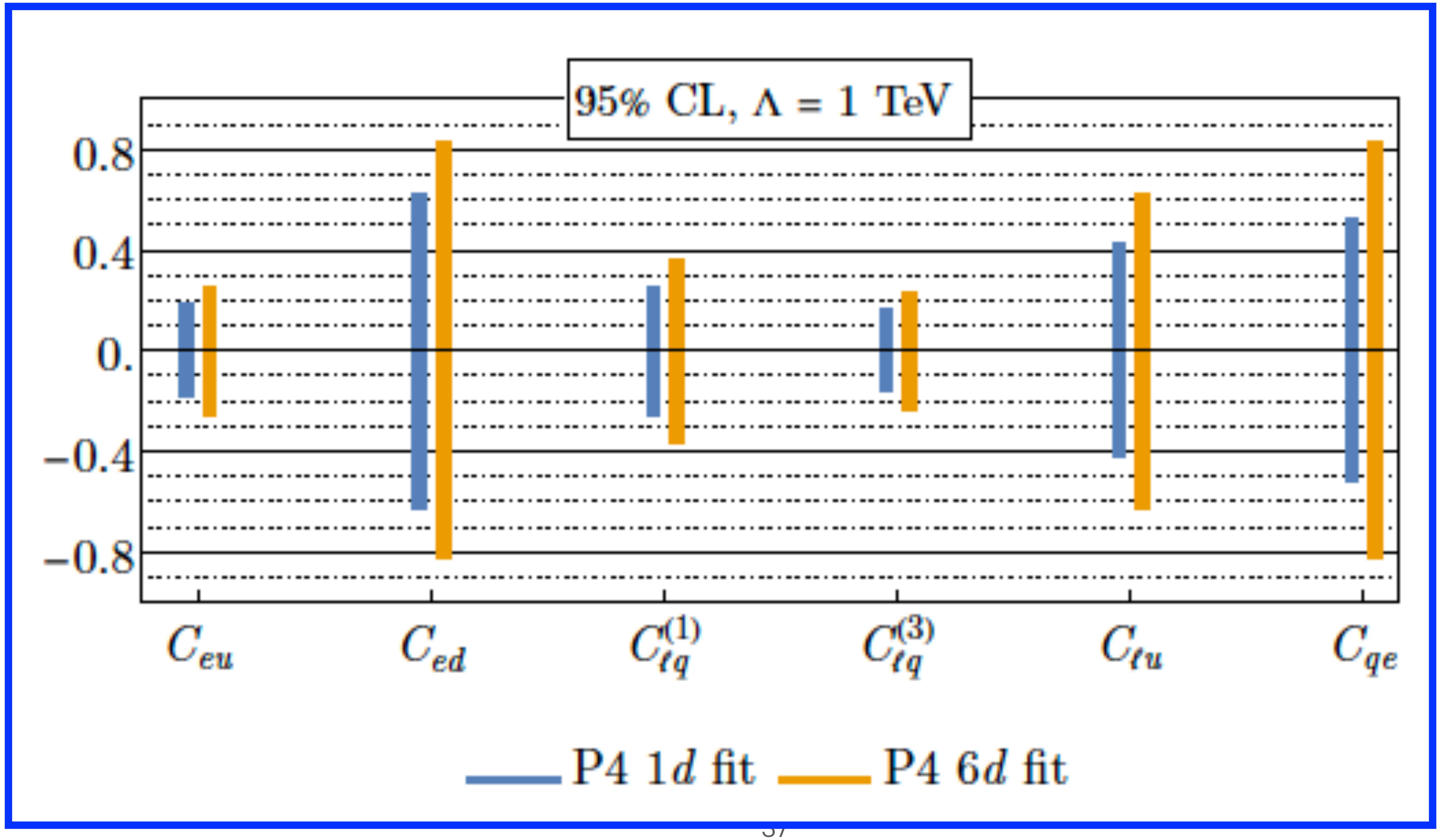

Multi-parameter fits

- We can turn on more Wilson coefficients to test for degeneracies and check for degradation of the bounds. Only slightly weaker bounds in a 6-dimensional fit. The EIC can probe the full parameter space of semi-leptonic four-fermion Wilson coefficients.

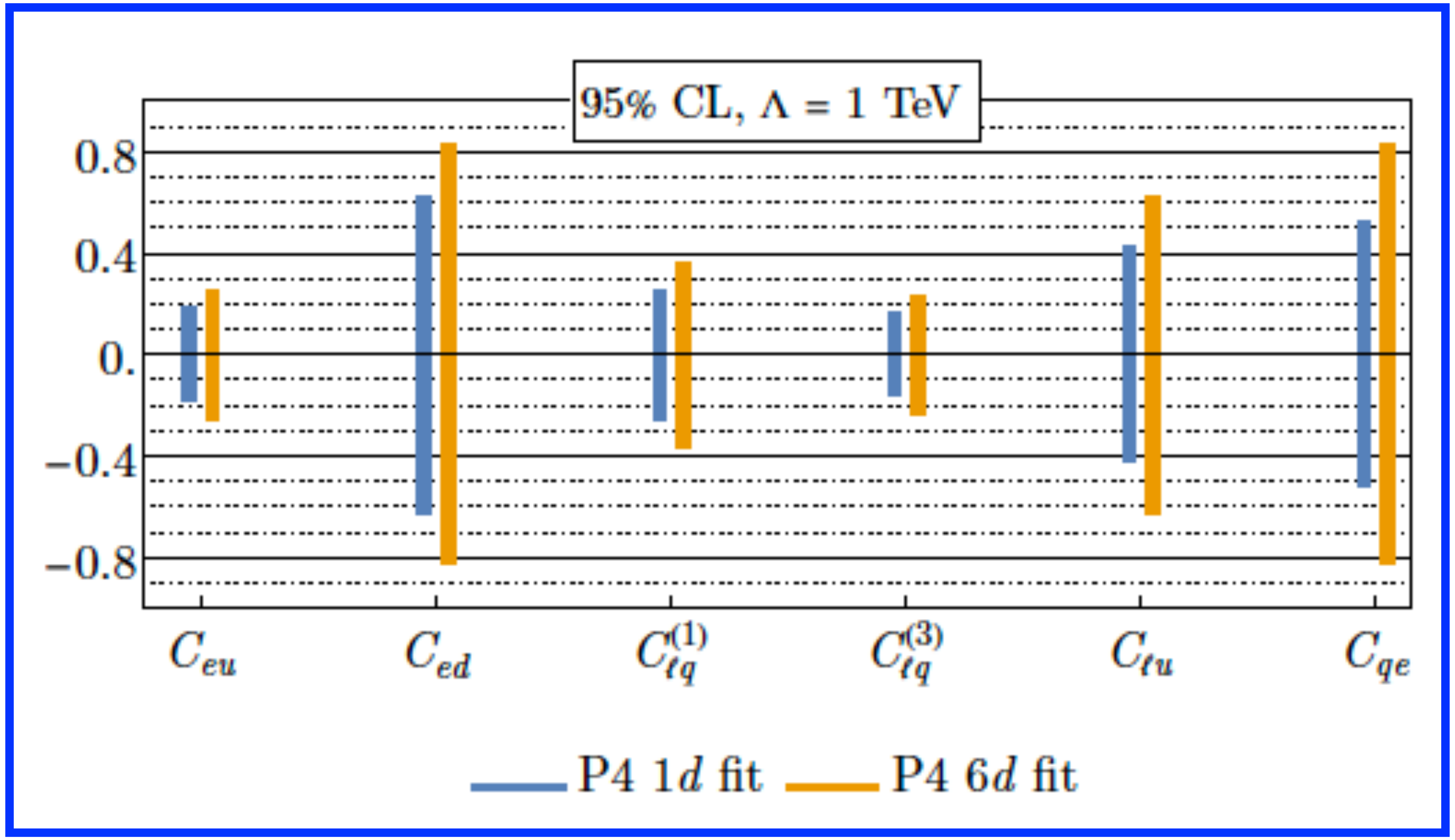

Compare to the LHC:

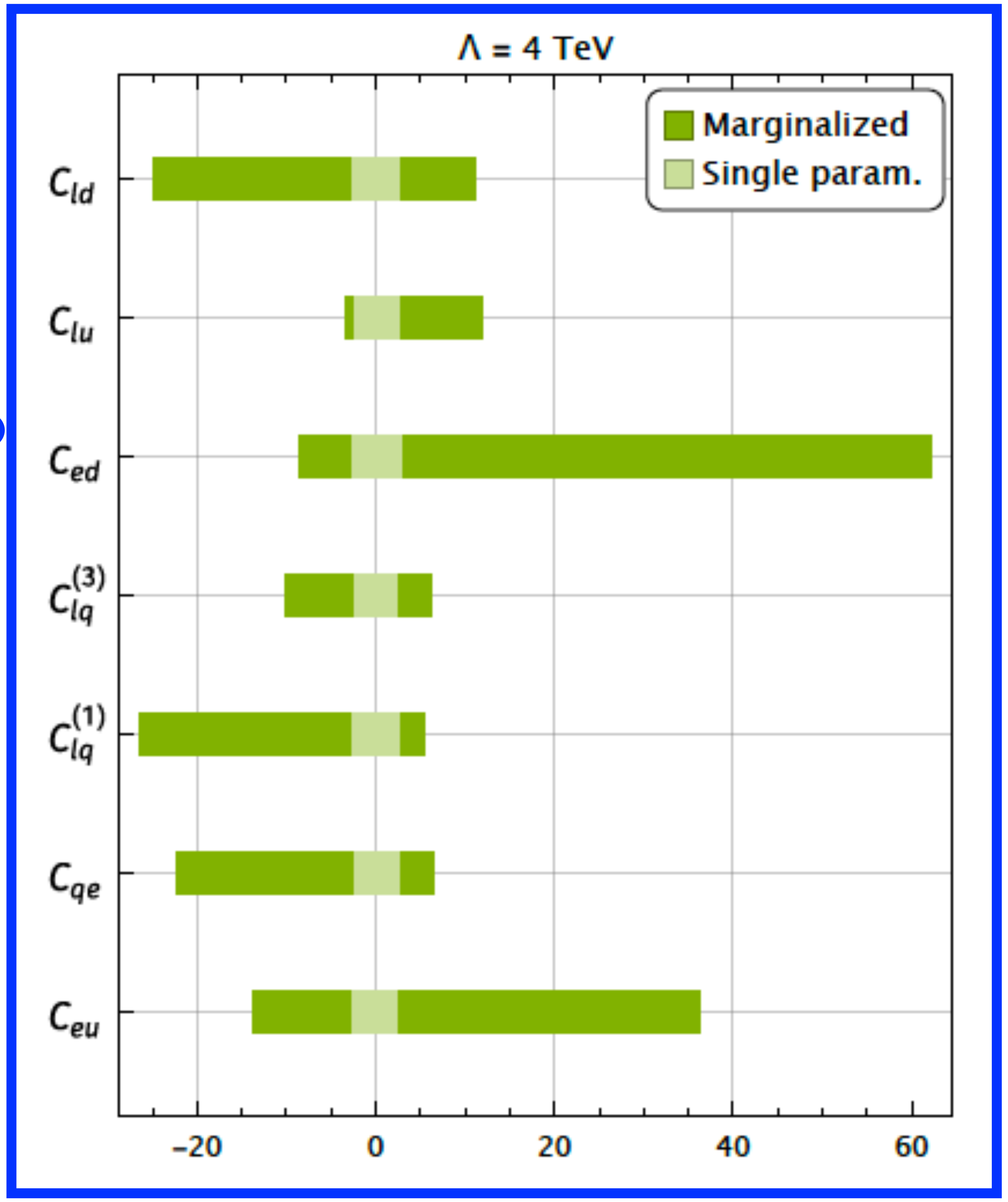

Future high-energy DIS experiments (LHeC/FCC-eh)

Comparison of future high-energy DIS machines

- Next we turn our attention to proposed future DIS machines such as the LHeC and the FCC-eh. We will compare the potential of the EIC with these future machines.

Experiment	Data set label	Data set configuration	Observable
LHeC	LHeC1	60 GeV $\times$ 1000 GeV e^-p, $P_\ell = 0$, $\mathcal{L} = 100$ fb^{-1}	σ_{NC}
	LHeC2	60 GeV $\times$ 7000 GeV e^-p, $P_\ell = -80\%$, $\mathcal{L} = 100$ fb^{-1}	
	LHeC3	60 GeV $\times$ 7000 GeV e^-p, $P_\ell = +80\%$, $\mathcal{L} = 30$ fb^{-1}	
	LHeC4	60 GeV $\times$ 7000 GeV e^+p, $P_\ell = +80\%$, $\mathcal{L} = 10$ fb^{-1}	
	LHeC5	60 GeV $\times$ 7000 GeV e^-p, $P_\ell = -80\%$, $\mathcal{L} = 1000$ fb^{-1}	
	LHeC6	60 GeV $\times$ 7000 GeV e^-p, $P_\ell = +80\%$, $\mathcal{L} = 300$ fb^{-1}	
	LHeC7	60 GeV $\times$ 7000 GeV e^+p, $P_\ell = 0\%$, $\mathcal{L} = 100$ fb^{-1}	
FCC-eh	FCCeh1	60 GeV $\times$ 50000 GeV e^-p, $P_\ell = -80\%$, $\mathcal{L} = 2$ ab^{-1}	σ_{NC}
	FCCeh2	60 GeV $\times$ 50000 GeV e^-p, $P_\ell = +80\%$, $\mathcal{L} = 0.5$ ab^{-1}	
	FCCeh3	60 GeV $\times$ 50000 GeV e^+p, $P_\ell = 0$, $\mathcal{L} = 0.2$ ab^{-1}	
EIC	D4	10 GeV $\times$ 137 GeV e^-D, $P_\ell = 80\%$, $\mathcal{L} = 100$ fb^{-1}	A_{PV}
	D5	18 GeV $\times$ 137 GeV e^-D, $P_\ell = 80\%$, $\mathcal{L} = 15.4$ fb^{-1}	
	P4	10 GeV $\times$ 275 GeV e^-p, $P_\ell = 80\%$, $\mathcal{L} = 100$ fb^{-1}	
	P5	18 GeV $\times$ 275 GeV e^-p, $P_\ell = 80\%$, $\mathcal{L} = 15.4$ fb^{-1}	
	ΔD4	The same as D4 but with $P_\ell = 0$ and $P_H = 70\%$	ΔA_{PV}
	ΔD5	The same as D5 but with $P_\ell = 0$ and $P_H = 70\%$	
	ΔP4	The same as P4 but with $P_\ell = 0$ and $P_H = 70\%$	
	ΔP5	The same as P5 but with $P_\ell = 0$ and $P_H = 70\%$	

Note different polarizations, lepton species (e+ vs e-). Will be important later!

LHeC, FCC-eh run scenarios taken from the literature. All three machines feature high luminosity, polarization

LHeC: a future high-energy DIS experiment

- **LHeC** (updated CDR: 2007.14491): a potential future high-energy DIS experiment based on the existing LHC experiment

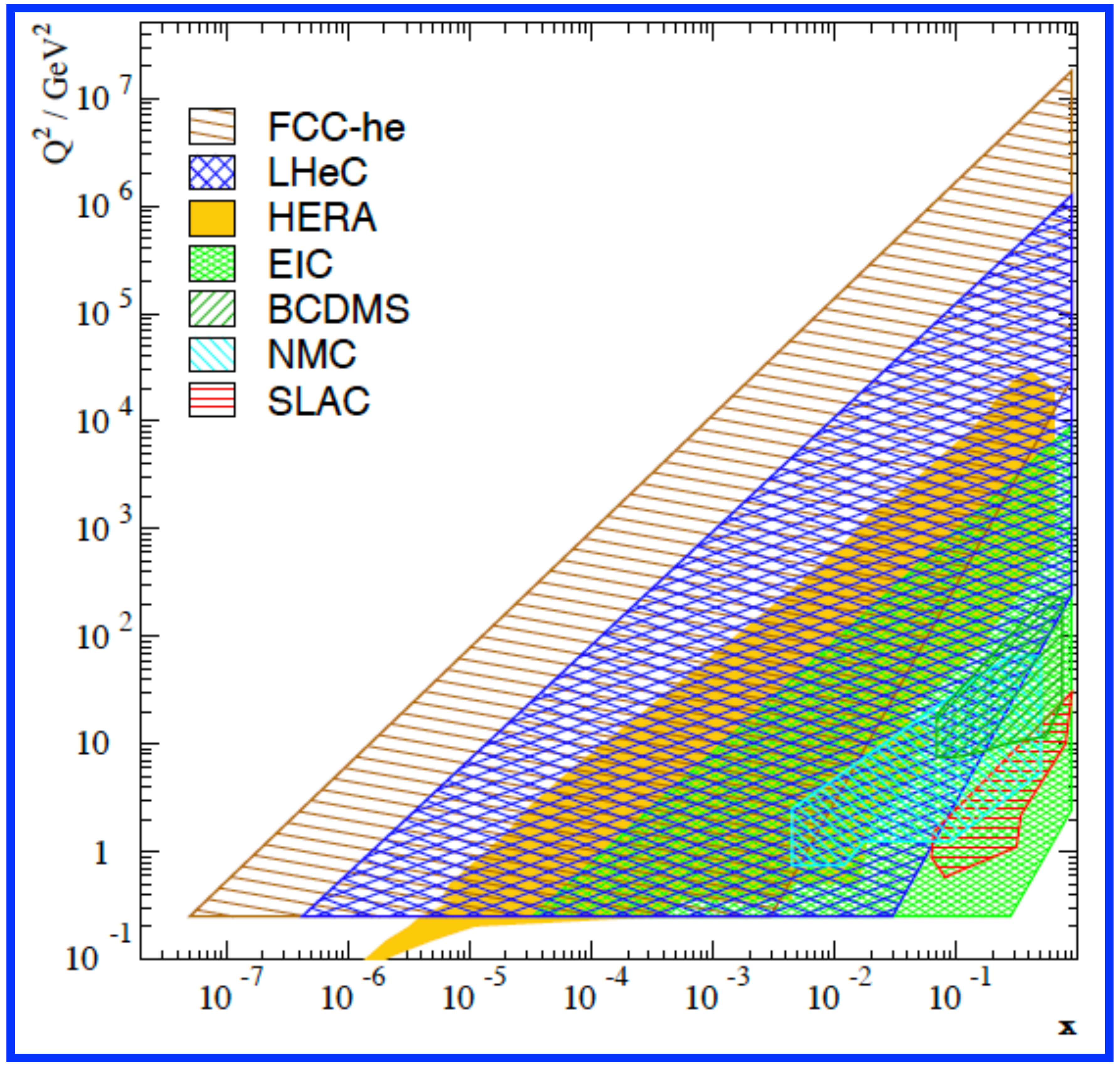

- Would feature a 50 GeV electron beam scattering off existing LHC proton/ion beams with a center-of mass energy reaching 1.5 TeV; concurrent operation with HL-LHC possible
- The integrated luminosity of such a machine could reach 1000 fb^{-1}
- Momentum transfers exceeding 1 TeV
- Increased coverage in the (x,Q^2) plane
- The possibility of polarizing the proton beam isn't considered, since the LHeC will reuse the LHC beam

FCC-eh: a second future high-energy DIS experiment

- **FCC-eh**: a proposed DIS experiment based upon a future circular collider complex at CERN

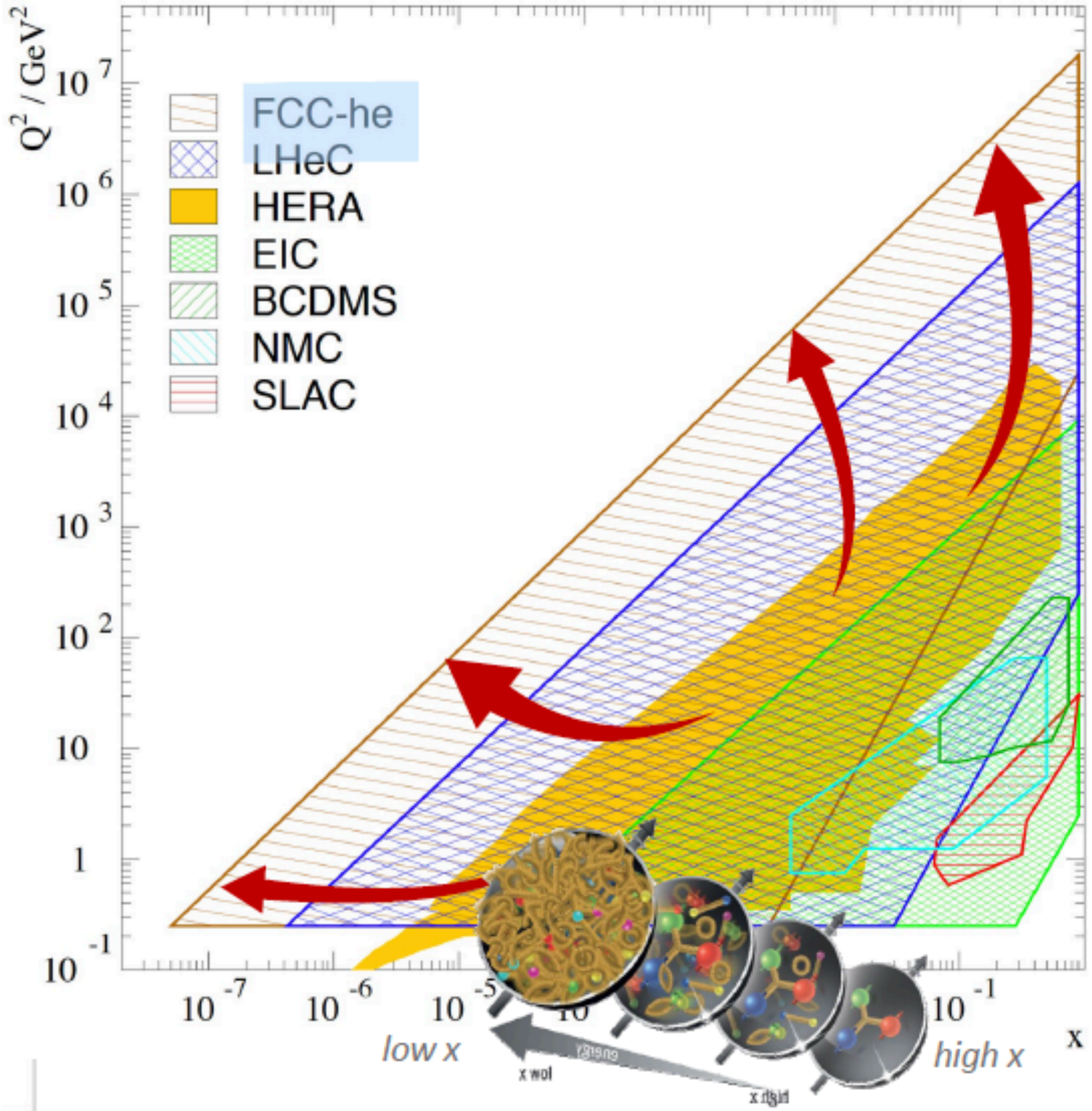

- Features a 60 GeV electron beam leading to a center-of mass energy of 3.5 TeV
- Up to several inverse attobarns of integrated luminosity
- Momentum transfers reaching 1.5 TeV
- Increased coverage in the (x,Q^2) plane

Error budgets for LHeC, FCC-eh

- Both future machines will be limited by systematic errors (purple lines in the plots below). Note that the estimated PDF errors (orange lines) are equal to or less than the systematic errors in most phase space; they will not be limiting factors for these analyses. NLO QCD is included, error from NNLO negligible.

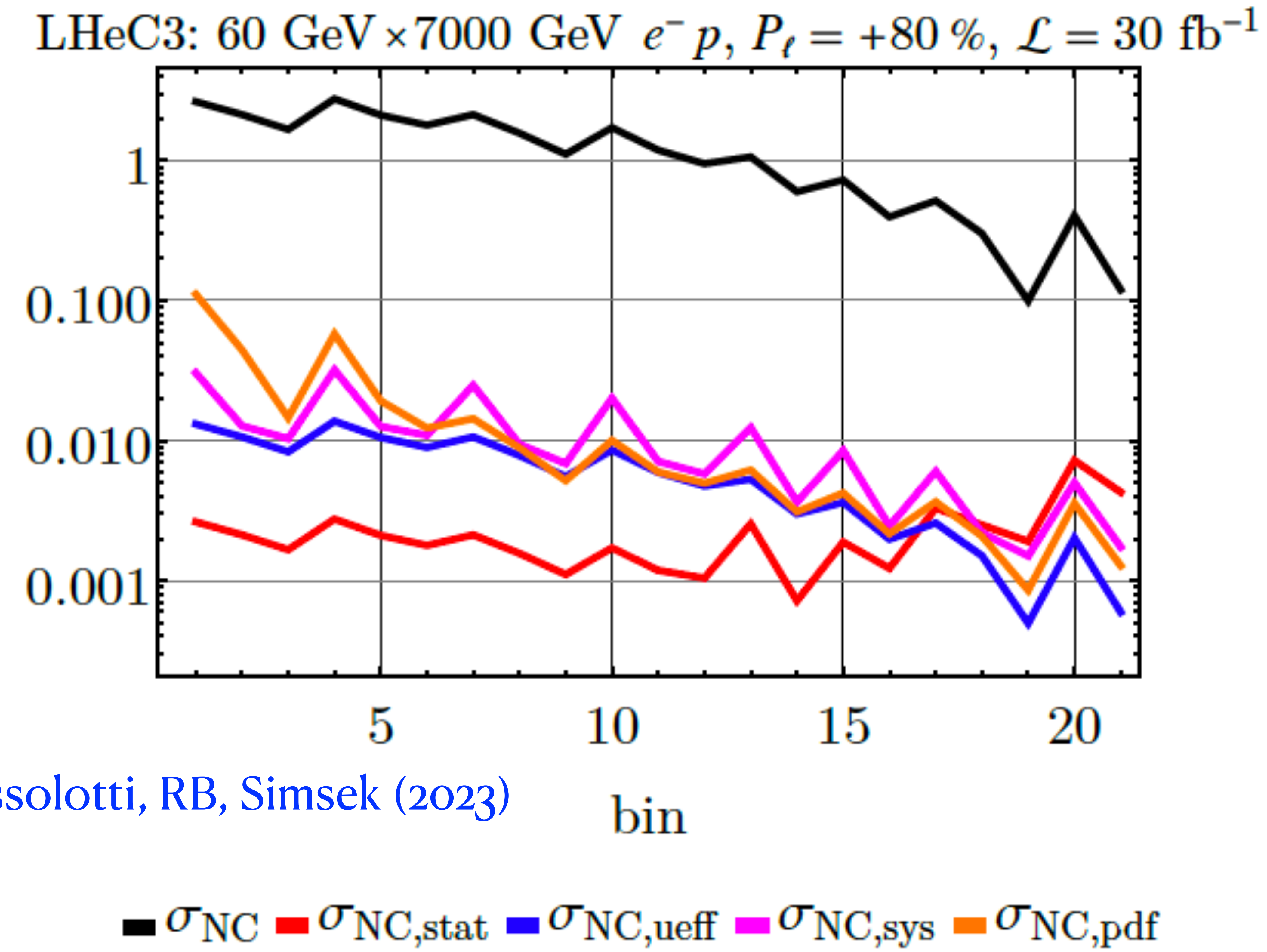

Bissolotti, RB, Simsek (2023)

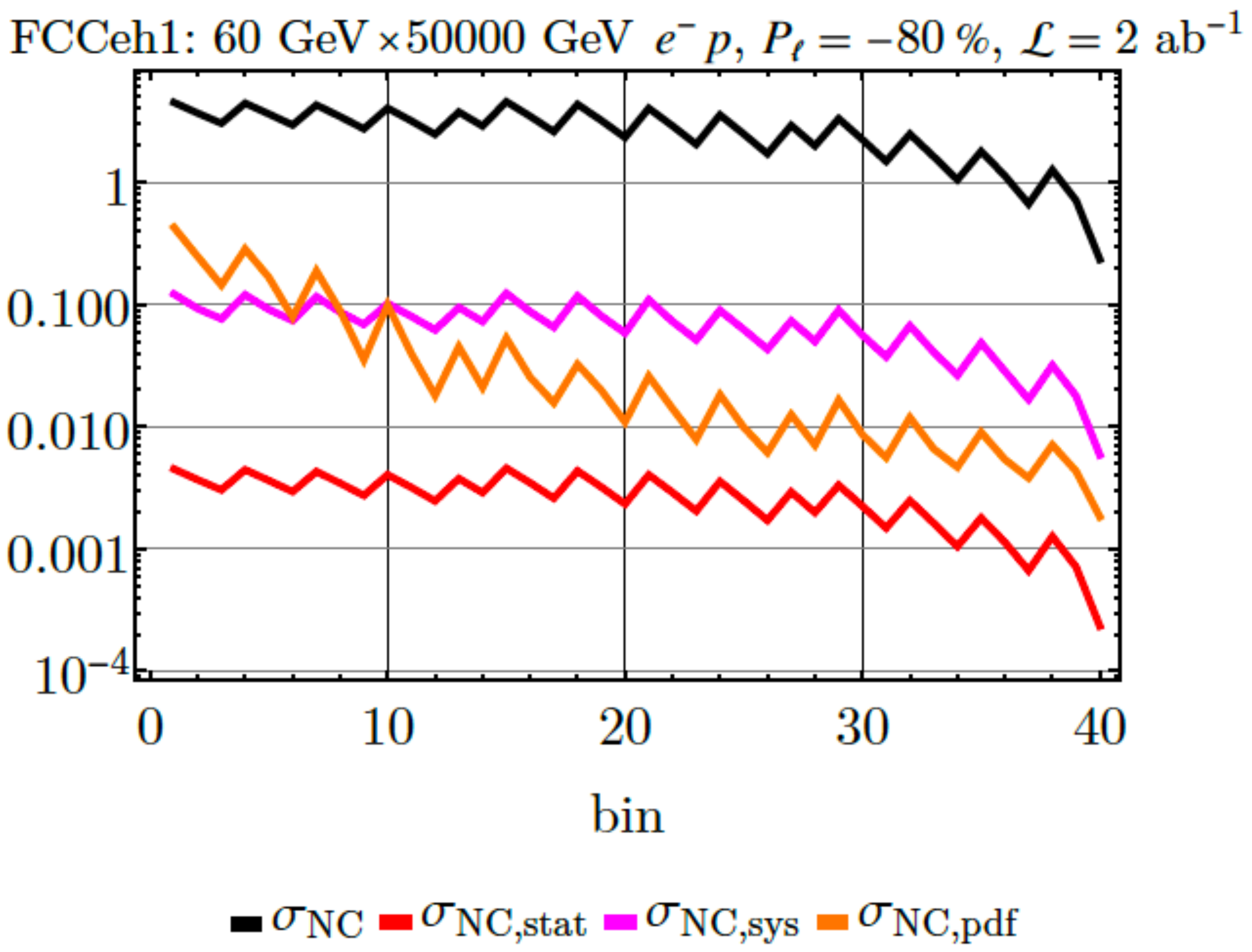

Marginalized constraints

- Note that future machines do not suffer from parameter space degeneracies like the LHC. To show this we focus on an example where the SMEFT corrections to three run scenarios (LHeC2, LHeC4, LHeC5) approximately vanish, still focusing on four-fermion interactions.

Bissolotti, RB, Simsek (2023)

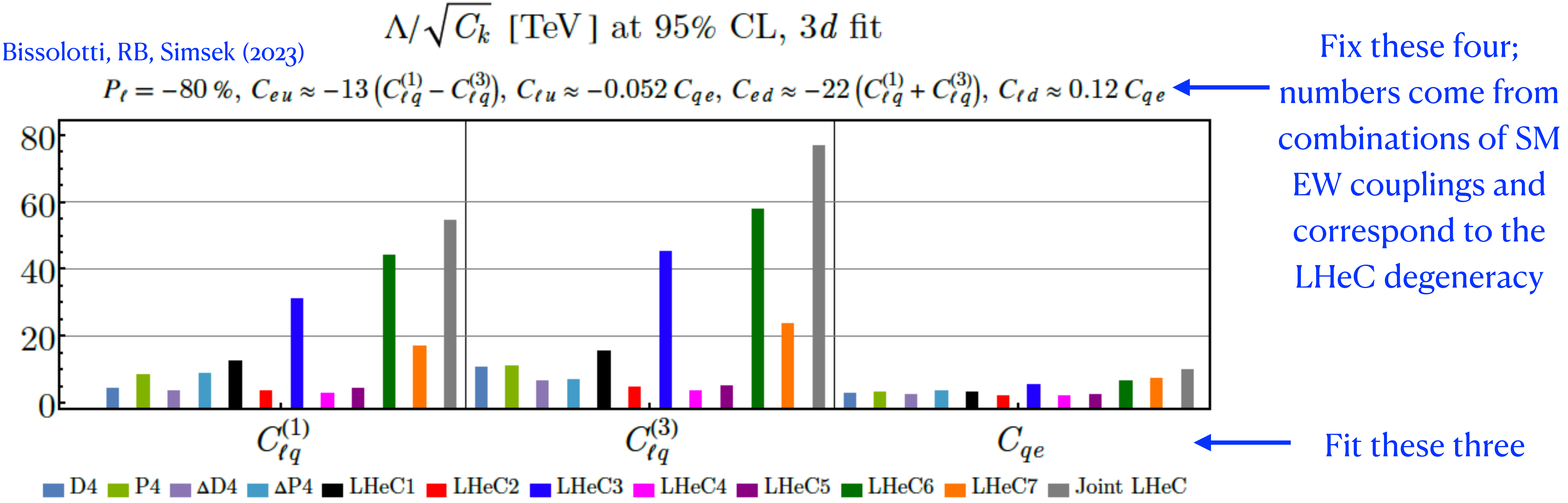

Marginalized constraints

Bissolotti, RB, Simsek (2023)

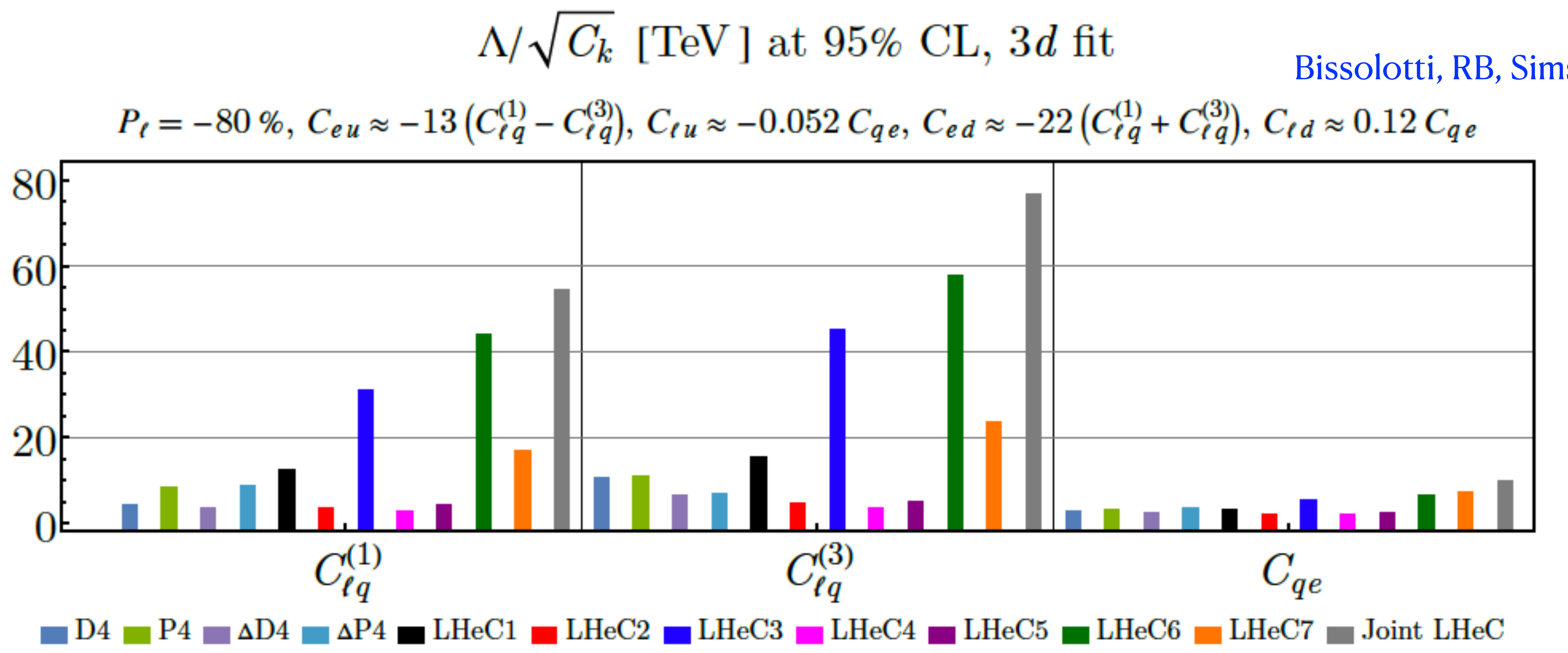

- Combined bounds on the effective UV scale from all LHeC runs reach 10 TeV for all three coefficients, 70 TeV for the strongest.
- Need all polarization, lepton species to cover the parameter space! No single LHeC run is the strongest for all three parameters.
- Not surprisingly, combined LHeC (and FCC-eh) bounds are far stronger than EIC bounds; higher energy and integrated luminosity.

Electroweak precision constraints

- The power of these future machines is so strong that we can improve upon the existing precision constraints on the ffV vertices driven primarily by LEP and SLC.

ffV		semi-leptonic four-fermion	
$C_{\varphi WB}$	$O_{\varphi WB} = (\varphi^\dagger \tau^I \varphi) W^I_{\mu\nu} B^{\mu\nu}$	$C^{(1)}_{\ell q}$	$O^{(1)}_{\ell q} = (\bar{\ell}\gamma_\mu \ell)(\bar{q}\gamma^\mu q)$
$C_{\varphi D}$	$O_{\varphi D} = (\varphi^\dagger D_\mu \varphi)^* (\varphi^\dagger D^\mu \varphi)$	$C^{(3)}_{\ell q}$	$(\bar{\ell}\gamma_\mu \tau^I \ell)(\bar{q}\gamma^\mu \tau^I q)$
$C^{(1)}_{\varphi \ell}$	$O^{(1)}_{\varphi \ell} = (\varphi^\dagger i \overleftrightarrow{D}_\mu \varphi)(\bar{\ell}\gamma^\mu \ell)$	C_{eu}	$O_{eu} = (\bar{e}\gamma_\mu e)(\bar{u}\gamma^\mu u)$
$C^{(3)}_{\varphi \ell}$	$O^{(3)}_{\varphi \ell} = (\varphi^\dagger i \overleftrightarrow{D}_\mu \tau^I \varphi)(\bar{\ell}\gamma^\mu \tau^I \ell)$	C_{ed}	$O_{ed} = (\bar{e}\gamma_\mu e)(\bar{d}\gamma^\mu d)$
$C_{\varphi e}$	$O_{\varphi e} = (\varphi^\dagger i \overleftrightarrow{D}_\mu \varphi)(\bar{e}\gamma^\mu e)$	$C_{\ell u}$	$O_{\ell u} = (\bar{\ell}\gamma_\mu \ell)(\bar{u}\gamma^\mu u)$
$C^{(1)}_{\varphi q}$	$O^{(1)}_{\varphi q} = (\varphi^\dagger i \overleftrightarrow{D}_\mu \varphi)(\bar{q}\gamma^\mu q)$	$C_{\ell d}$	$O_{\ell d} = (\bar{\ell}\gamma_\mu \ell)(\bar{d}\gamma^\mu d)$
$C^{(3)}_{\varphi q}$	$O^{(3)}_{\varphi q} = (\varphi^\dagger i \overleftrightarrow{D}_\mu \tau^I \varphi)(\bar{q}\gamma^\mu \tau^I q)$	C_{qe}	$O_{qe} = (\bar{q}\gamma_\mu q)(\bar{e}\gamma^\mu e)$
$C_{\varphi u}$	$O_{\varphi u} = (\varphi^\dagger i \overleftrightarrow{D}_\mu \varphi)(\bar{u}\gamma^\mu u)$		
$C_{\varphi d}$	$O_{\varphi d} = (\varphi^\dagger i \overleftrightarrow{D}_\mu \varphi)(\bar{d}\gamma^\mu d)$		
$C_{\ell\ell}$	$O_{\ell\ell} = (\bar{\ell}\gamma_\mu \ell)(\bar{\ell}\gamma^\mu \ell)$		

We turn on the full 17 operators that contribute to DIS at tree-level in the EW couplings

Electroweak precision constraints

- The power of these future machines is so strong that we can improve upon the existing precision constraints on there ffV vertices driven primarily by LEP and SLC.

ffV		semi-leptonic four-fermion	
$C_{\varphi WB}$	$O_{\varphi WB} = (\varphi^\dagger \tau^I \varphi) W^I_{\mu\nu} B^{\mu\nu}$	$C^{(1)}_{\ell q}$	$O^{(1)}_{\ell q} = (\bar{\ell}\gamma_\mu \ell)(\bar{q}\gamma^\mu q)$
$C_{\varphi D}$	$O_{\varphi D} = (\varphi^\dagger D_\mu \varphi)^* (\varphi^\dagger D^\mu \varphi)$	$C^{(3)}_{\ell q}$	$(\bar{\ell}\gamma_\mu \tau^I \ell)(\bar{q}\gamma^\mu \tau^I q)$
$C^{(1)}_{\varphi \ell}$	$O^{(1)}_{\varphi \ell} = (\varphi^\dagger i \overleftrightarrow{D}_\mu \varphi)(\bar{\ell}\gamma^\mu \ell)$	C_{eu}	$O_{eu} = (\bar{e}\gamma_\mu e)(\bar{u}\gamma^\mu u)$
$C^{(3)}_{\varphi \ell}$	$O^{(3)}_{\varphi \ell} = (\varphi^\dagger i \overleftrightarrow{D}_\mu \tau^I \varphi)(\bar{\ell}\gamma^\mu \tau^I \ell)$	C_{ed}	$O_{ed} = (\bar{e}\gamma_\mu e)(\bar{d}\gamma^\mu d)$
$C_{\varphi e}$	$O_{\varphi e} = (\varphi^\dagger i \overleftrightarrow{D}_\mu \varphi)(\bar{e}\gamma^\mu e)$	$C_{\ell u}$	$O_{\ell u} = (\bar{\ell}\gamma_\mu \ell)(\bar{u}\gamma^\mu u)$
$C^{(1)}_{\varphi q}$	$O^{(1)}_{\varphi q} = (\varphi^\dagger i \overleftrightarrow{D}_\mu \varphi)(\bar{q}\gamma^\mu q)$	$C_{\ell d}$	$O_{\ell d} = (\bar{\ell}\gamma_\mu \ell)(\bar{d}\gamma^\mu d)$
$C^{(3)}_{\varphi q}$	$O^{(3)}_{\varphi q} = (\varphi^\dagger i \overleftrightarrow{D}_\mu \tau^I \varphi)(\bar{q}\gamma^\mu \tau^I q)$	C_{qe}	$O_{qe} = (\bar{q}\gamma_\mu q)(\bar{e}\gamma^\mu e)$
$C_{\varphi u}$	$O_{\varphi u} = (\varphi^\dagger i \overleftrightarrow{D}_\mu \varphi)(\bar{u}\gamma^\mu u)$		
$C_{\varphi d}$	$O_{\varphi d} = (\varphi^\dagger i \overleftrightarrow{D}_\mu \varphi)(\bar{d}\gamma^\mu d)$		
$C_{\ell\ell}$	$O_{\ell\ell} = (\bar{\ell}\gamma_\mu \ell)(\bar{\ell}\gamma^\mu \ell)$		

Existing single-parameter constraints on the ffV Wilson coefficients are quite strong; can future DIS experiments improve upon these?

Dawson, Giardino (2019)

C_k	95% CL, $\Lambda = 1$ TeV
$C^{(1)}_{\varphi\ell}$	$[-0.043, 0.012]$
$C^{(3)}_{\varphi\ell}$	$[-0.012, 0.0029]$
$C_{\varphi e}$	$[-0.013, 0.0094]$
$C^{(1)}_{\varphi q}$	$[-0.027, 0.043]$
$C^{(3)}_{\varphi q}$	$[-0.011, 0.014]$
$C_{\varphi u}$	$[-0.072, 0.091]$
$C_{\varphi d}$	$[-0.16, 0.060]$
$C_{\varphi WB}$	$[-0.0088, 0.0013]$

Electroweak precision constraints

- We consider the full 17-dim marginalized fit and show 2-dim projections below for all three machines: EIC, LHeC, FCC-eh. We take the EWPO fit from J.Ellis et al (2012.02779).

Bissolotti, RB Simsek (2023)

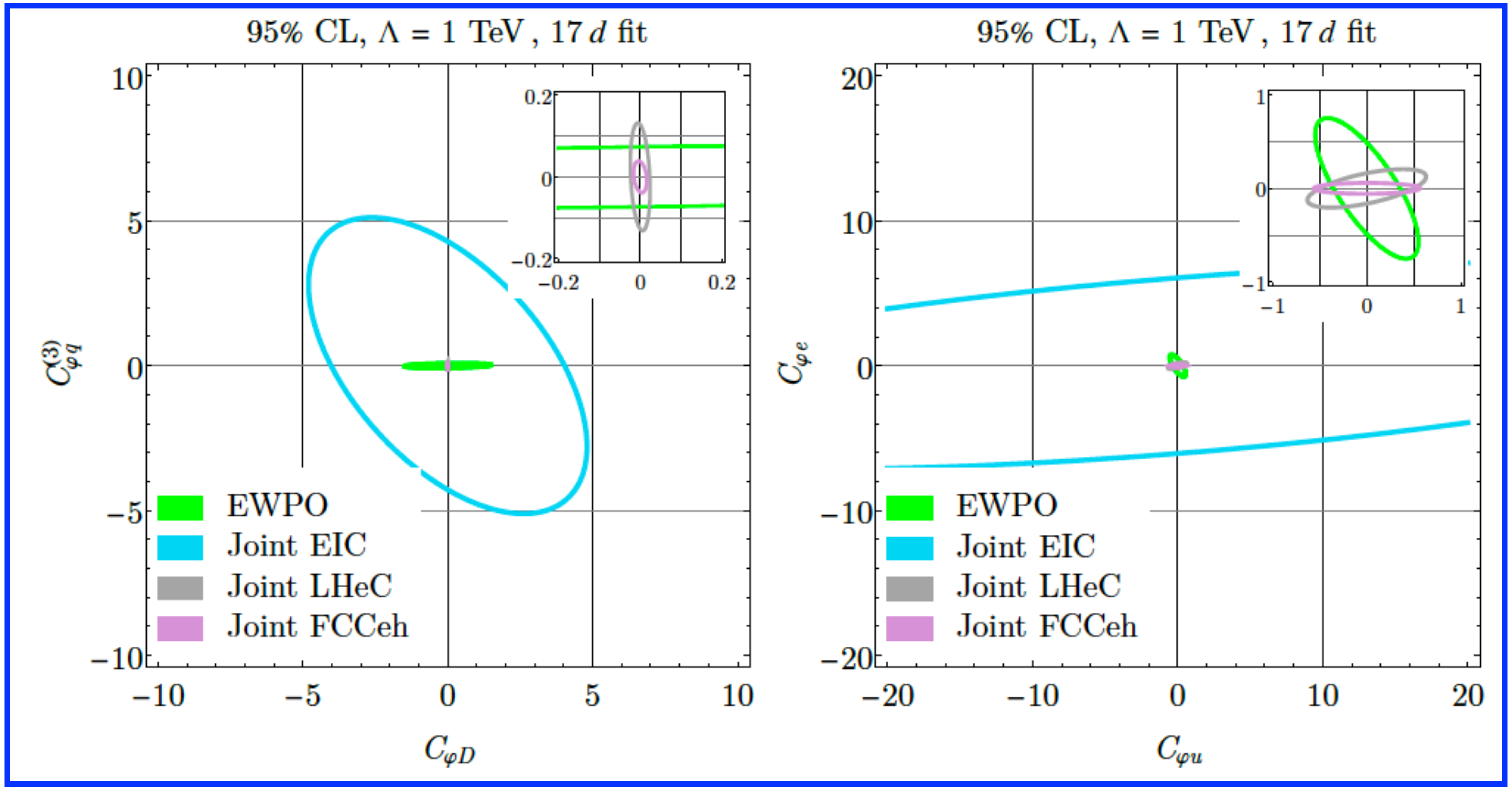

Two example projections of the full 17-dim fit. The FCC-eh can significantly improve on EWPO constraints!

Low-energy experiments

Low-energy SMEFT probes

- We have shown that high invariant-mass LHC measurements can entangle dim-6 and dim-8 effects. Future high-energy DIS machines are less sensitive to dim-8 due to their lower momentum transfers. Their enhanced sensitivity to SMEFT effects comes from polarization and anticipated small errors.
- Low-energy experiments have much smaller centre of mass energy, and dimension-8 effects completely decouple. Several future high-precision parity-violating electron scattering (PVES) experiments are planned.

$(ee)(qq)$

	$[c^{(3)}_{\ell q}]_{1111}$	$[c_{\ell q}]_{1111}$	$[c_{\ell u}]_{1111}$	$[c_{\ell d}]_{1111}$	$[c_{eq}]_{1111}$	$[c_{eu}]_{1111}$	$[c_{ed}]_{1111}$
CHARM	-80 ± 180	700 ± 1800	370 ± 880	-700 ± 1800	x	x	x
APV	27 ± 19	1.6 ± 1.1	3.4 ± 2.3	3.0 ± 2.0	-1.6 ± 1.1	-3.4 ± 2.3	-3.0 ± 2.0
QWEAK	7.0 ± 12	-2.3 ± 4.0	-3.5 ± 6.0	-7 ± 12	2.3 ± 4.0	3.5 ± 6.0	7 ± 12
PVDIS	-8 ± 12	24 ± 35	38 ± 48	-77 ± 96	-77 ± 96	-12 ± 17	24 ± 35
SAMPLE	-8 ± 45	x	-17 ± 90	17 ± 90	x	-17 ± 90	17 ± 90
$d_j \to u\ell\nu$	0.38 ± 0.28	x	x	x	x	x	x
LEP-2	3.5 ± 2.2	-42 ± 28	-21 ± 14	42 ± 28	-18 ± 11	-9.0 ± 5.7	18 ± 11

$(\mu\mu)(qq)$

	$[c^{(3)}_{\ell q}]_{2211}$	$[c_{\ell q}]_{2211}$	$[c_{\ell u}]_{2211}$	$[c_{\ell d}]_{2211}$	$[c_{eq}]_{2211}$	$[c_{eu}]_{2211}$	$[c_{ed}]_{2211}$
PDG ν_μ	20 ± 15	4 ± 21	18 ± 19	-20 ± 37	x	x	x
SPS	0 ± 1000	0 ± 3000	0 ± 1500	0 ± 3000	40 ± 390	-20 ± 190	40 ± 390
$d_j \to u\ell\nu$	-0.4 ± 1.2	x	x	x	x	x	x

Falkowski, Gonzalez-Alonso, Mimouni (2017)

Existing low-energy experiments already provide constraints on semi-leptonic four-fermion operators

Low-energy SMEFT probes

- We have shown that high invariant-mass LHC measurements can entangle dim-6 and dim-8 effects. Future high-energy DIS machines are less sensitive to dim-8 due to their lower momentum transfers. Their enhanced sensitivity to SMEFT effects comes from polarization and anticipated small errors.
- Low-energy experiments have much smaller centre of mass energy, and dimension-8 effects completely decouple. Several future high-precision parity-violating electron scattering (PVES) experiments are planned.

$(ee)(qq)$

	$[c^{(3)}_{\ell q}]_{1111}$	$[c_{\ell q}]_{1111}$	$[c_{\ell u}]_{1111}$	$[c_{\ell d}]_{1111}$	$[c_{eq}]_{1111}$	$[c_{eu}]_{1111}$	$[c_{ed}]_{1111}$
CHARM	-80 ± 180	700 ± 1800	370 ± 880	-700 ± 1800	x	x	x
APV	27 ± 19	1.6 ± 1.1	3.4 ± 2.3	3.0 ± 2.0	-1.6 ± 1.1	-3.4 ± 2.3	-3.0 ± 2.0
QWEAK	7.0 ± 12	-2.3 ± 4.0	-3.5 ± 6.0	-7 ± 12	2.3 ± 4.0	3.5 ± 6.0	7 ± 12
PVDIS	-8 ± 12	24 ± 35	38 ± 48	-77 ± 96	-77 ± 96	-12 ± 17	24 ± 35
SAMPLE	-8 ± 45	x	-17 ± 90	17 ± 90	x	-17 ± 90	17 ± 90
$d_j \to u \ell \nu$	0.38 ± 0.28	x	x	x	x	x	x
LEP-2	3.5 ± 2.2	-42 ± 28	-21 ± 14	42 ± 28	-18 ± 11	-9.0 ± 5.7	18 ± 11

$(\mu\mu)(qq)$

	$[c^{(3)}_{\ell q}]_{2211}$	$[c_{\ell q}]_{2211}$	$[c_{\ell u}]_{2211}$	$[c_{\ell d}]_{2211}$	$[c_{eq}]_{2211}$	$[c_{eu}]_{2211}$	$[c_{ed}]_{2211}$
PDG ν_μ	20 ± 15	4 ± 21	18 ± 19	-20 ± 37	x	x	x
SPS	0 ± 1000	0 ± 3000	0 ± 1500	0 ± 3000	40 ± 390	-20 ± 190	40 ± 390
$d_j \to u \ell \nu$	-0.4 ± 1.2	x	x	x	x	x	x

Falkowski, Gonzalez-Alonso, Mimouni (2017)

Operators are normalized according to C_i/v^2 where v is the Higgs vev, and in most cases the limits are sub-TeV. Are there future higher-precision low-energy experiments that can probe this parameter space?

Low-energy SMEFT probes

- Several such future experiments are planned with ultra high-intensity beams, and with anticipated extremely small experimental and theoretical errors.

$$A_{PV} = \frac{\sigma_R - \sigma_L}{\sigma_R + \sigma_L}$$

The planned measurement for these experiments is the polarization asymmetry, the difference in right- and left-handed electrons

SoLID: $2<Q^2<10$ GeV^2, electron-deuteron scattering (JLab)

P2: 155 MeV electrons off hydrogen/carbon targets (Mainz)

Extremely small momentum transfers; sensitive only to dim-6, helping remove degeneracies in LHC fits!

Exquisite precision and consequently strong probes of SMEFT parameters expected!

Example fit to LHC+P2 data

- We will consider an example fit to LHC invariant mass data and to the expected P2 errors.

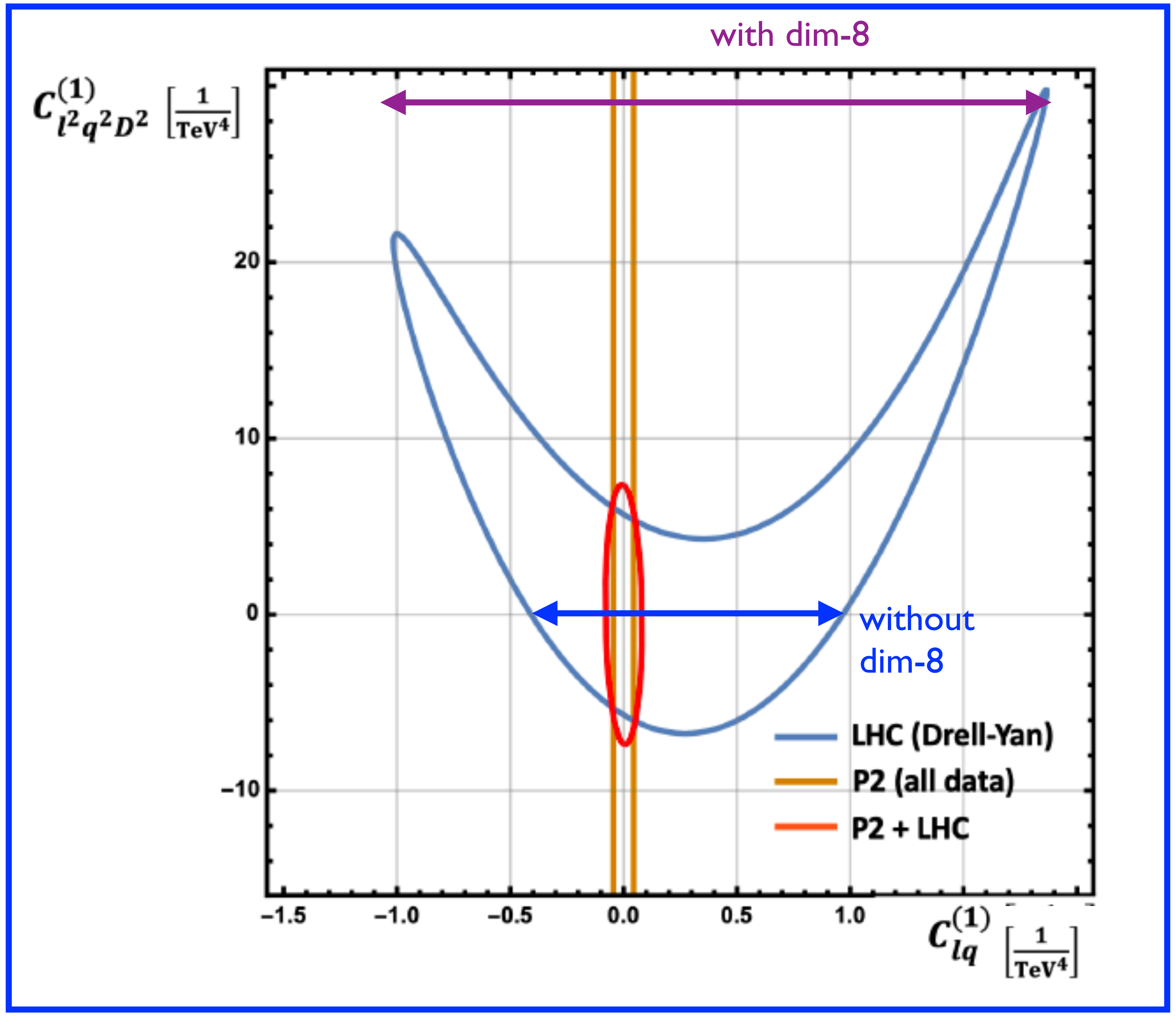

RB, Petriello, Wiegand (2021)

Assume couplings between left-handed quarks and leptons for this example.

Blue ellipse: LHC alone; turning on dim-8 increases the allowed range of the dim-6 Wilson coefficient by a factor of 2. Minimum effective dim-8 scales allowed in blue region are $\Lambda/\sqrt[4]{C}\approx 1.5$ TeV

Example fit to LHC+P2 data

- We will consider an example fit to LHC invariant mass data and to the expected P2 errors.

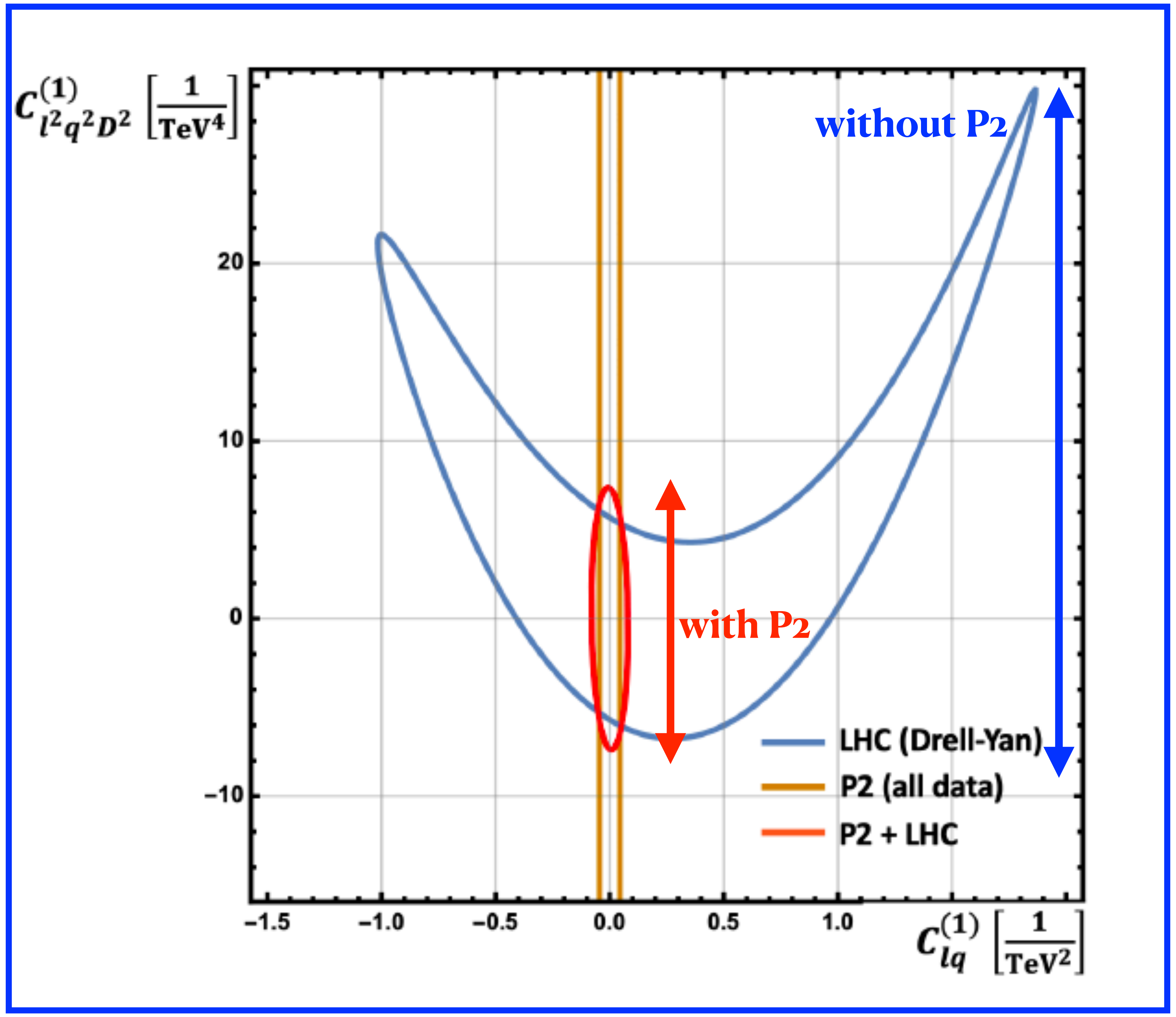

RB, Petriello, Wiegand (2021)

Assume couplings between left-handed quarks and leptons for this example.

Red ellipse: joint fit with P2; P2 severely constrains the allowed range of the dim-6 coefficient, freeing the LHC Drell-Yan data to constrain the dim-8 effect

Future low-energy parity violating measurements will play an important role in global fits of the SMEFT parameter space.

Conclusions

- The current experimental landscape suggests that the coming decade will require increasingly precise indirect searches in order to find hints of deviation from the SM.
- The SMEFT framework is ideal for organizing and interpreting these searches.
- The EIC is capable of powerful indirect probes of BSM effects difficult to access at the LHC due to its ability to polarize both beams.
- We have shown that the EIC can remove degeneracies in the four-fermion sector of the SMEFT that the LHC cannot distinguish.
- LHeC and FCCeH will further advance searches for heavy new physics.
- Looking forward to a rich and exciting future DIS program!